ADAPTIVE TETRODOTOXIN-RESISTANCE IN GARTER SNAKE SODIUM CHANNELS

by

Chong Hyun Lee
Bachelor of Science, Simon Fraser University, 2007

THESIS SUBMITTED IN PARTIAL FULFILLMENT OF
THE REQUIREMENTS FOR THE DEGREE OF

MASTER OF SCIENCE

In the
Department of Biomedical Physiology and Kinesiology

SIMON FRASER UNIVERSITY

Fall, 2009

APPROVAL

Name: **Chong Hyun Lee**

Degree: **Master of Science**

Title of Thesis: **Adaptive Tetrodotoxin-Resistance in Garter Snake Sodium Channels.**

Examining Committee:

Chair: **Dr. Matthew White**
Associate Professor

_____

Dr. Peter C. Ruben
Senior Supervisor
Professor and Director

_____

Dr. Glen Tibbits
Supervisor
Professor

_____

Dr. Charles Krieger
Supervisor
Professor

_____

Dr. Tom Claydon
External Examiner
Assistant Professor

Date Defended/Approved: _____December 4, 2009_____

Declaration of Partial Copyright Licence

ABSTRACT

Tetrodotoxin (TTX) is a neurotoxin that specifically binds to voltage gated sodium channels (Na_V). TTX binding physically blocks the flow of sodium ions through Na_V, thereby preventing action potential generation and propagation. TTX has different binding affinities for different Na_V isoforms. These differences are imparted by amino acid substitutions in positions within, or proximal to, the TTX binding site in the channel pore. The garter snake *Thamnophis sirtalis* has evolved TTX-resistance over the course of an arms race, allowing some populations of snakes to feed on tetrodotoxic newts, including *Taricha granulosa*. We tested the properties of Na_V with TTX resistance found in garter snake populations. We observed some surprising changes in gating properties and ion selectivity of the TTX resistant Na_V. These results suggest TTX resistance comes at a cost to performance caused by changes in the biophysical properties and/or ion selectivity of the TTX resistant Na_V.

Keywords: Tetrodotoxin; TTX; Voltage Gated Sodium Channel; NaV; Sodium Currents; Garter Snake; Gating Property; Ion Selectivity.

DEDICATION

I would like to dedicate my work to my parents who supported me through all my life and my family: lovely wife Seo-Hyun and my son Joel.

ACKNOWLEDGEMENTS

First, I would like to thank Dr. Peter C. Ruben who introduced the world of voltage-gated sodium channels to me. He has inspired and supported me throughout my master's program. In addition, I would like to thank my good colleagues Dave K. Jones and Dr. Yuriy Y. Vilin for their support and help. Without them, my master's years would have been very dry and boring. Many thanks to all the members of the Molecular Cardiac Physiology Group for their great work and support. Finally, I would like to thank NSERC for funding my project.

TABLE OF CONTENTS

Approval ii
Abstract iii
Dedication iv
Acknowledgements v
Table of Contents vi
List of Figures viii
List of Tables ix

1: Introduction 1
1.1 Opening 1
1.2 The specific aims of the present thesis: 3
1.2.1 Test voltage dependent gating of mutants. 3
1.2.2 Test conductance and ion selectivity of mutants. 3

2: Background: literature review 4
2.1 Voltage-gated sodium channel structure 4
2.1.1 Voltage-gated sodium channel genes 9
2.1.2 Voltage-gated sodium channels in pain pathways 10
2.1.3 Neurotoxin binding sites in Voltage-gated sodium channel. 11
2.2 Tetrodotoxin 14
2.3 Adaptive evolution of elevated resistance to TTX in Na_V 16
2.3.1 TTX resistance in puffer fish 17
2.3.2 STX resistance in softshell clams 18
2.3.3 TTX-resistance in garter snake 19

3: Materials and Methods 24
3.1 cDNA and mRNA Preparation 24
3.2 Oocytes Preparation and Injection 25
3.3 Electrophysiology 26
3.4 Data Analysis 30

4: Results 31
4.1 Biophysical Properties of Channel Gating. 31
4.1.1 Activation 33
4.1.2 Fast Inactivation 35
4.1.3 Slow Inactivation 37
4.2 Ion Selectivity of Channel 39

5: Discussion 43
5.1 Effect on the Voltage Dependent Gating of Na_V 44

5.2 Effect on the Ion selectivity and Permeability of Na_V.....50

6: Conclusion 53

Reference List 54

LIST OF FIGURES

Figure 1. Transmembrane diagram of α-subunit of Na_V. 5
Figure 2. Molecular Structure of Tetrodotoxin. 14
Figure 3. Localities and relationships of *Thamnophis sirtalis*. 21
Figure 4. Amino acid sequence differences of four snake populations. 23
Figure 5. Gating Properties of Wild Type $Na_V1.4$ with or without β subunit. 32
Figure 6. Family of Na_V Current Traces. 34
Figure 7. Peak Na_V current vs. Voltage Graphs. 34
Figure 8. Activation of sodium channels. 35
Figure 9. Steady-State Fast inactivation raw current traces 36
Figure 10. Steady-State Fast Inactivation of sodium channels. 36
Figure 11. Steady-State Slow inactivation raw current traces 38
Figure 12. Steady-State Slow Inactivation of sodium channels. 38
Figure 13. Family of current traces recorded using Li^+ external solution. 41
Figure 14. Normalized current and voltage relationship under different external solutions 41
Figure 15. Permeability ratio of the cations 42

LIST OF TABLES

Table 1. Mammalian Na_V isoforms and their TTX sensitivity. 10
Table 2. Neurotoxins that target the Na_V channels and their corresponding receptor sites. 13
Table 3. Composition of external solutions. 30
Table 4. Effect of Summary of β subunit in $Na_V1.4$ gating properties. 33
Table 5. Biophysical parameters of the channel activation. 33
Table 6. Biophysical parameters of steady-state fast inactivation of the channels 37
Table 7. Biophysical parameters of steady-state slow inactivation of the channels. 39
Table 8. Summary of Reversal Potential and Permeability Ratio. 42

1: INTRODUCTION

1.1 Opening

Voltage-gated sodium channels (Na_v) are large, membrane-bound protein complexes composed of a heterotetrameric α-subunit and one or more smaller β-subunits [1-3]. Sodium channels are expressed in a variety of excitable tissues including nerve, muscle and heart. Activation (opening) of Na_V regulates the flow of sodium ions across the membrane of a cell and, therefore, controls action potential generation and propagation. The α-subunit is composed of four homologous domains (DI–DIV); each domain contains six α-helical transmembrane segments (S1–S6) [15]. The α-subunit is responsible for voltage sensitivity and ion permeation and selectivity. The β-subunits (33~37kDa) serve important roles in cell adhesion, signal transduction, channel expression, and modulate voltage dependence and kinetics of Na_V gating [16, 17]. To date, nine mammalian Na_v genes (or paralogs), and a related tenth gene, have been identified [4]. Different members of Na_V isoforms are expressed in different types of excitable tissues.

Tetrodotoxin (TTX) is a naturally occurring potent neurotoxin that selectively occludes Na_v in nerve and muscle tissues, thereby inhibiting the propagation of APs and paralyzing nerve and muscle function [5, 6]. It was first found in the puffer fish family Tetraodontidae, from which its name is derived, and soon after was discovered in octopus, goby fish, frogs, newts and more [7].

These organisms are adapted to carry TTX as a defence against predation. Some tradeoffs, however, were unavoidable. Na_V in puffer fish and newts have been reported to carry mutations in various sites of different channel isoforms [8-12]. Mutations in the channel can affect the rate of nerve impulse, sensory transduction, and muscle contraction and, therefore, the animals' fitness. Predators of TTX-carrying organisms have co-evolved TTX-resistance via mutations in Na_v, presumably as a result of the selective pressure imposed by TTX carrying prey [13, 14]. For example, the garter snake *Thamnophis sirtalis* has evolved TTX-resistance over the course of an arms race, allowing some populations of snakes to feed on tetrodotoxic newts, especially including *Taricha granulosa* [13]. A similar phenomenon has also been observed in some populations of softshell clams (*Mya arenaria*), which have developed resistance to saxitoxin (STX), a TTX-related neurotoxin [14]. Amino acid sequence analysis of skeletal Na_V of the garter snake revealed that unique amino acid substitutions in the highly-conserved pore region of domain IV that controls gating and selectivity of the channel are the basis of TTX-resistance in the garter snake population. The pore region plays a critically important role in channel gating and selectivity, and it is reasonable to hypothesize that these properties may have been altered as a consequence of the amino acid substitutions. My thesis is designed to test this hypothesis by studying the gating properties and selectivity of Na_V from the garter snake *Thamnophis sirtalis*. The answers to this question will help us understand whether there are biophysical, and perhaps organismic, tradeoffs for the advantage of TTX resistance. In addition, this study will examine

the importance of a conserved portion of the channel for proper channel function and skeletal muscle physiology.

1.2 The specific aims of the present thesis:

1.2.1 Test voltage dependent gating of mutants.

Test the hypothesis that amino acid substitutions that impart TTX resistance in snake skeletal muscle sodium channels result in changes in voltage dependent gating.

1.2.2 Test conductance and ion selectivity of mutants.

Test the hypothesis that amino acid substitutions that impart TTX resistance in snake skeletal muscle sodium channels result in changes in conductance and ion selectivity.

2: BACKGROUND: LITERATURE REVIEW

2.1 Voltage-gated sodium channel structure

A voltage gated sodium channel is comprised of a highly processed α-subunit (260kDa) and one or more smaller accessory β-subunits (33~37kDa). The β-subunits are important in modifying voltage dependency and kinetics in Na_v gating [15]. In addition, they play important roles in cell adhesion, signal transduction, and channel expression at the plasma membrane [16]. The α-subunit is formed from four homologous domains (DI–DIV) and each domain contains six α-helical transmembrane segments (S1–S6) [17]. Transmembrane segments are connected through small intracellular and extracellular loops, and larger intracellular loops connect homologous domains (Figure 1) [18].

The α-subunit is important in channel function, including voltage sensitivity and ion selectivity. The S4 transmembrane segments of the α-subunit have been shown to be the voltage sensors in Na_v, as in other voltage-gated ion channels [17]. They include positively charged arginine and lysine residues at every third amino acid position. Depolarization of the membrane triggers the positively charged S4's to translocate toward the extracellular side of the cell membrane and initiates the channel activation [19]. This movement of charge within the protein and primarily confined to the intramembrane region of S4's, gives rise to gating currents and is suggested to mediate channel gating [20]. Neutralization of the positive charges in S4 transmembrane segments of all four domains results

in altered channel gating [21, 22].

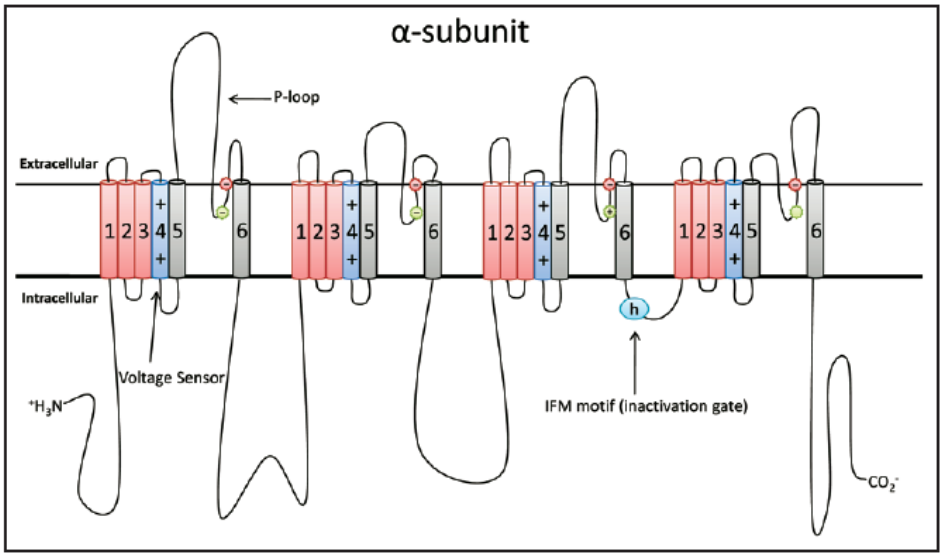

Figure 1. Transmembrane diagram of α-subunit of Na_V.

The α-subunit is formed from four homologous domains with six α-helical transmembrane segments in each domain. The polypeptide chains connect subunits and domains. S4 segments are voltage sensors and IFM motif in intracellular loop between DIII and DIV act as inactivation gate. P-loops of all four domains and S6 segments forms extracellular and intracellular ends of the pore and TTX binds to the selectivity filter in P-loops (outer EEDD; inner DEKA).

The voltage sensor is also associated with the voltage dependence of channel inactivation [23, 24]. The outward movement of the voltage sensor opens the channel and also exposes an intracellular binding site for the IFM motif of the inactivation gate. The inactivation particle is a triad of hydrophobic residues, isoleucine, phenylalanine and methionine (IFM), located in the intracellular DIII-DIV linker. The IFM triad quickly inactivates the channel by blocking the pore [1-3]. This rapid closing process of the channel is called fast inactivation (FI). FI is responsible for terminating action potential and leaves the

channel refractory for some time after repolarization. Sodium channels enter the fast-inactivated state in a voltage-dependent transition [25]. Changes in voltage dependence of FI in Na_V contribute to diseases including long QT syndrome type 3 in cardiac myocytes, critical illness myopathy, paramyotonia congenita and hyperkalemic periodic paralysis in skeletal muscle [25, 26]. In contrast, slow inactivation is apparent after prolonged or repeated depolarizations of the channel and does not apparently involve the IFM fast inactivation particle; it is biophysically, pharmacologically, and molecularly different from fast inactivation [27, 28]. The structural underpinnings of SI, however, are poorly understood [27, 28]. In *Shaker* K^+ channels, C-type (slow) inactivation is associated with pore constriction related to structural rearrangements in the P-regions as well as the gating motion of voltage sensors [29]. Similarly in Na_V, it is proposed that prolonged and repeated depolarizations may change the interaction between the S4 voltage sensor and the pore, resulting a constriction or collapse of the ion permeation pathway [30, 31]. Nonetheless, the impairment of the channels to enter the slow inactivated state in Na_V accentuates the muscle membrane depolarization that lead to skeletal muscle paralysis including hyperkalemic periodic paralysis and paramyotonia congenita [32]. Slow inactivation, in combination with closed-state fast inactivation, play a crucial role in membrane excitability by contributing to the regulation of resting sodium channel availability [27, 33, 34].

The ion permeation pathway of Na_V is a critical structural determinant of normal channel function. Due to its crucial role, the pore region of the channel is

highly conserved. Studies using site-directed mutagenesis in the pore forming P-regions have shown that mutations in the pore region produce a marked decrease in sodium ion conductance and TTX-sensitivity [13, 35-39], and have an effect on voltage-dependent gating in activation [40, 41] and slow inactivation [33, 34]. The traditional view of the Na_v conducting pathway is a single pore, similar to the crystal structure of the pore-forming part of the KcsA bacterial K^+ channel, which carries the characteristic selectivity of voltage-gated K^+ channels [42]. The three-dimensional structure of a KcsA bacterial K^+ channel revealed that the channel is composed of four homologous subunits and each subunit contains two α-helical transmembrane segments, M1 and M2. [42]. Conducting pathway is lined by the four subunits and the highly conserved TXXTXGYG sequence found in the P-loops that link the four sets of M1 and M2 form narrow ion-selective region of the channel through lining their backbone carbonyls [42]. The carbonyls form several ion binding sites, one external site and several internal sites and they also serve essential roles in ion dehydration. The structure of the KcsA K^+ channel also revealed that two dehydrated permeant ions residing in the narrow region of the permeation pathway, while a third hydrated ion is found in the water-filled cavity in the internal vestibule. The amino acid sequence of pore lining P-regions are well conserved in various K^+ channels indicating that they share a similar structure and, therefore, the ion permeation pathway of the KcsA K^+ channel is used as a template.

Similarly, in Na_V, the S5 and S6 membrane-spanning segments as well as the P-loops that link the S5-S6 transmembrane of all four domains are proposed

to form the ion permeation pathway of the channel. The narrow extracellular vestibule of the pore is formed by the P-regions whereas the wider intracellular vestibule of the pore is lined by the S5 and S6 segments [35, 43, 44]. Ions entering the outer vestibule of Na_V must pass through the narrow selectivity filter before they can enter the inner pore of the channel. The selectivity filter is composed of amino acid residues in the P-regions that form two negatively charged narrow rings. Four negatively charged amino acids residues, glutamate (DI), glutamate (DII), aspartate (DIII), and aspartate (DIV), form the outer ring, and aspartate (DI), glutamate (DII), lysine (DIII) and alanine (DIV) form the inner ring [35]. Interaction between these amino acid residues from P-loops stabilizes the pore structure of the channel [45]. Amino acid residues of the P-regions also form pore-helix and β-strand that stabilize the outer vestibule and produce binding pocket for TTX [46]. In contrast to the traditional view, Sato *et al.,* [47] using cryo-electron microscopy technique, proposed that the 3D structure of Na_V to consist of a bell shaped outer surface, square-shaped bottom and a hemi-spherical top with four small pores on the extracellular side of the cell. These four small pores are connected to a central body that diverges to four outlet pores in the intracellular side and twisting and untwisting of the central cavity corresponds to the closed and open states of the channel ("*twist-sprinkler*" model) [48]. This multi-pore structure of the channel allows the massive influx of sodium channels during rapidly changing membrane potential.

2.1.1 Voltage-gated sodium channel genes

To date, nine mammalian Na_v proteins have been identified and functionally expressed ($Na_v1.1$, $Na_v1.2$, $Na_v1.3$, $Na_v1.4$, $Na_v1.5$, $Na_v1.6$, $Na_v1.7$, $Na_v1.8$, and $Na_v1.9$), and a tenth protein (Na_x) has been recognized as a related protein that does not encode a voltage-gated sodium channel [4]. These isoforms are all greater than 50% identical in amino acid sequence in the transmembrane and extracellular domains and the functional properties are relatively similar [4]. All of the nine sodium channel isoforms are therefore suggested to be members of a single family. As expected, some isoforms are more closely related to one another than to others. This variation in relation appears to also correlate with chromosomal location. $Na_V1.1$, $Na_V1.2$, $Na_V1.3$, and $Na_V1.7$ are highly TTX-sensitive and their genes are localized on human chromosome 2q23-24 [35, 36, 49-51]. The genes encoding Na_v localized on human chromosome 2 are mainly expressed in the central and peripheral neurons. $Na_V1.4$ is localized in chromosome 17, and that encoding $Na_V1.6$ is located in chromosome 12. $Na_V1.4$ and $Na_V1.6$ are both TTX-sensitive channels and predominantly expressed in skeletal muscle and in the central nervous system, respectively [52, 53]. $Na_V1.5$, $Na_V1.8$, and $Na_V1.9$ are TTX-resistant and their genes are located on human chromosome 3p21-24 [39, 54-56]. The gene encoding $Na_V1.5$ is primarily expressed in the heart, and $Na_V1.8$ and $Na_V1.9$ are mainly found in dorsal root ganglion (DRG) neurons. TTX-resistant channels from chromosome 3 have a unique amino acid substitution at the pore forming P-loop of DI; a non-aromatic amino acid is found at site 401 in TTX-resistant channels, whereas TTX-sensitive channels have an aromatic ring amino acid at the site. This substitution reduces

TTX-sensitivity [38, 39, 56, 57]. The Na_V isoforms expressed in a particular excitable tissue thus determines its TTX sensitivity (Table 1).

Table 1. Mammalian Na_V isoforms and their TTX sensitivity.

Channel	Gene	TTX sensitivity	Distribution
$Na_V1.1$	SCN1A	EC_{50} = 6 nM[38]	CNS
$Na_V1.2$	SCN2A	EC_{50} = 18 nM[27,30]	CNS
$Na_V1.3$	SCN3A	EC_{50} = 4 nM[39]	CNS
$Na_V1.4$	SCN4A	EC_{50} = 25 nM[41]	skeletal muscle
$Na_V1.5$	SCN5A	EC_{50} = 5.7 μM[43]	heart
$Na_V1.6$	SCN8A	EC_{50} = 6 nM[42]	CNS
$Na_V1.7$	SCN9A	EC_{50} = 24.5 nM[40]	PNS(DRG)
$Na_V1.8$	SCN10A	EC_{50} = 60 μM[45]	PNS(DRG)
$Na_V1.9$	SCN11A	EC_{50} = 40 μM[33]	PNS(DRG)

*EC_{50}, median effective concentration; CNS, central nerve system; PNS, peripheral nerve system; DRG, dorsal root ganglion.

2.1.2 Voltage-gated sodium channels in pain pathways

Voltage-gated sodium channels play a crucial role in signal transduction sensory neurons, whose somata lie within the dorsal root ganglia (DRG). Specifically, the TTX-resistant channels $Na_V1.8$ and $Na_V1.9$ are located in pain-sensing peripheral neurons (nociceptors) and are important factors in physiological and pathophysiological pain sensation, and Na_V blockers have been clinically used as analgesics for both normal and neuropathic pain for many years. The chronic-constriction-injury model used in neuropathic pain studies shows that peripheral nerve injury up-regulates expression levels of TTX-sensitive $Na_V1.3$ in damaged peripheral neurons within the DRG [58-60]. Normally, $Na_V1.3$ is preferentially localized in central neurons of adults and its

expression is greater during embryonic development than in adults (Table 1). One of the key properties of $Na_V1.3$ is a marked increase in the rate of recovery from fast inactivation compared to TTX-resistant channels, $Na_V1.8$ and 1.9, normally present in nociceptors [61]. The abnormal expression of $Na_V1.3$, and its more rapid recovery from inactivation, suggests that it may play an important part in sustaining high frequency APs in chronic pain [62]. In fact, reducing expression of $Na_V1.3$ in nociceptors using anti-sense oligodeoxynucleotides, resulted in decreased hypersensitivity of DRG neurons, and attenuated associated pain [60]. Low dose TTX has been shown to decrease thermal and mechanical hyper-responsiveness in a chemotherapy-induced neuropathic pain model [62]. Although abnormal properties of nociceptors are caused by various additional factors, and although there is not yet a full understanding of all the mechanisms of neuropathic pain, TTX may potentially be a good analgesic intervention for peripheral pain hypersensitivity involving TTX-sensitive Na_V isoforms.

2.1.3 Neurotoxin binding sites in voltage-gated sodium channel.

Na_V are targets for several groups of neurotoxins that alter channel gating and permeation properties by binding to various receptor sites. Neurotoxins bind to Na_V with high affinity and specificity providing powerful tools to study the structure and the function of sodium channels [63]. Nine different neurotoxin receptor sites have been identified on Na_V (Table 2) [64]. The water soluble heterocyclic tetrodotoxin and saxitoxin and the peptide μ-conotoxin bind to the outer pore region of the channel (site 1) and block the Na^+ flux through the permeation pathway of the channel. The lipid soluble grayanotoxin, the alkaloids

veratridine and batrachotoxin are gating modifier neurotoxins that bind to receptor site 2 and brevetoxins and ciguatoxins bind to receptor site 5 [63]. The intramembrane receptor sites 2 and 5 are distinct from the pore or voltage sensor, however, the lipid soluble neurotoxins that bind to these sites enhance sodium channel activity through allosteric interactions that cause a shift in activation to more negative membrane potentials and a block of inactivation [65, 66]. This suggests that neurotoxin binding to a receptor site can induce conformational changes that subsequently alter the equilibrium between the open and the closed/inactivated states [63]. DDT and analogs and pyrethroids, and local anesthetics bind to intramembrane receptor sites 7 and 9, respectively, causing negative shift of activation and altered ion permeation of the channel [64]. Polypeptide gating modifier neurotoxins those bind to extracellular receptor sites 3 and 6 include α-scorpion and sea anemone toxins, and δ-conotoxins, respectively. These toxins slow or block sodium channel inactivation [63]. Similarly, goniopora and *conus striatus* toxins are inactivation gating modifiers that slow inactivation through increased sodium ion permeability, thereby prolonging the action potential. However, these toxins do not competitively bind to receptor site 3 with α-scorpion toxins suggesting a distinct binding sites for these toxins (site 8) [64]. Another group of scorpion neurotoxins, β-scorpions, bind to extracellular receptor site 4 and induce a hyperpolarizing shift in activation as well as a reduction in the peak sodium current amplitude [67].

Table 2. Neurotoxins that target the Na_V channels and their corresponding receptor sites.

Receptor Site	Putative location	Neurotoxin	Physiological effect
Site 1	P-regions of DI, DII, DIII and DIV	Tetrodotoxin Saxitoxin μ-Conotoxin	Pore blocker
Site 2	DI:S6, DII:S6	Batrachotoxin Veratridine	Persistent activation Depolarization of resting potential
	DIII: S6 DIV:S6	Aconitine Grayanotoxin	Repetitive firings
Site 3	DIV:S3-S4 DI:S3-S4 Loop	α-Scorpion toxins Sea anemone toxins	Slowed inactivation
Site 4	DII:S3-S4 Loop	β-Scorpion toxins	Enhanced activation; repetitive firings
Site 5	DI:S6 DIV:S5	Brevetoxins Ciguatoxins	Enhanced activation and block of inactivation
Site 6	DIV:S3-S4	δ-Conotoxins	Slowed inactivation
Site 7	? DI-S6 DII-S6 DIII-S6	Kalkitoxin DDT and analogs, Pyrethroids	Inhibitor, not a pore blocker Persistent activation gating; depolarization of resting potentials; repetitive firings
Site 8	? ?	Goniopora Conus striatus toxin	Inactivation gating modifier Slowed inactivation
Site 9	DI-S6 DIII-S6 DIV-S6	Local anesthetics, Anticonvulsants, Antidepressants	Inhibition of Na^+ permeability

This table was adapted from [64] and [63].

2.2 Tetrodotoxin

TTX is known as an extremely potent inhibitor of sodium currents in nerve and muscle. TTX is a low-molecular weight neurotoxin with a highly unusual chemical structure [7]. It consists of a positively charged guanidinium group and a pyrimidine ring with six hydroxyl groups at the C-4, C-6, C-8, C-9, C-10 and C-11 position (Figure 2).

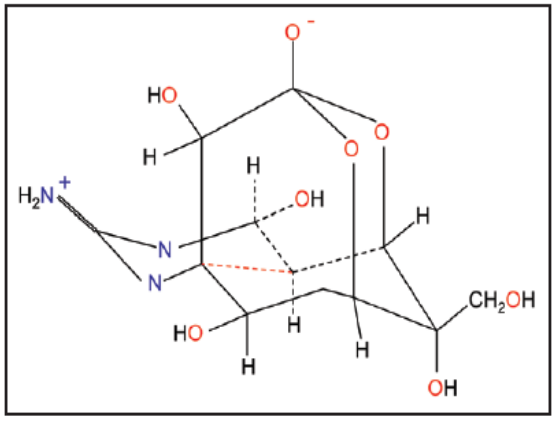

Figure 2. Molecular Structure of Tetrodotoxin.

TTX is predominantly isolated from the ovary and liver of puffer fish, and it has been detected in a remarkably wide range of organisms including fish, amphibians, arthropods, nematodes, echinoderms, molluscs, dinoflagellate and bacteria. The occurrence and distribution of TTX among a wide variety of organisms gave rise to speculation that TTX and its derivatives originated from symbiotic microorganisms. Indeed, a number of bacteria have been shown to produce TTX including the genera *Aeromonas* and *Alteromonas*, *Escherichia*

coli, Photobacterium phosphoreum, Plesiomonas shigelloides, Pseudomonas sp. and some *Vibrio sp*. (for a review see refs. [5-7]).

Site-directed mutagenesis experiments [35, 36], photoaffinity labelling [68, 69] and molecular modelling studies [46, 70] suggested that TTX binds to the neurotoxin receptor site located at the outer pore of Na_V. In addition, the inhibition of toxin binding by pH titration [71], carboxyl-modifying reagents [72], and some monovalent cations, divalent metal ions, and protons [73] supported the idea that the guanidinium group and the hydroxyls of TTX interact with the pore region of Na_V. The guanidinium group of TTX is proposed to form an ion-pair with negatively charged functional groups located in P-loops of DI (Asp-384, Glu-387) and DII (Glu-942), while the hydroxyl groups C9 and C10, and C11 of TTX form hydrogen bonds with Glu-945 in DII and Asp-1532 in DIV, respectively [70, 74, 75]. TTX binding to the pore sterically and/or electrostatically occludes sodium ion transport into the cell, leading to inhibition of AP generation and propagation. TTX binding consequently causes conduction block in muscle and nerves, and leads to diaphragm paralysis and death from respiratory failure.

The binding affinity of the channel for TTX is affected by changes in electrostatic interactions between TTX and the amino acid side chain lining of the pore. Neutralizing the negatively charged residues in the P-loops such as glutamine acid at 387, 942 and 945 and aspartic acid at 384 and 1532 caused marked decrease in TTX-sensitive channels [35, 36, 75]. Altering the shape of the selectivity filter region of the pore affects the TTX-sensitivity of the channel [38, 39, 57]. Substitution of an aromatic ring residue to a non-aromatic ring

residue at 401 in DI of TTX-sensitive channel isoforms produced substantial reduction in TTX-sensitivity while the TTX-resistant channel isoforms gained TTX-sensitivity by substituting an aromatic ring residue to the same site [38, 39, 57]. A strong non-bonded interaction between the aromatic ring and the non-polar surface of TTX is proposed to be hindered by the substitution [70]. The substitution is also proposed to distort the positions of critical channel residues in the selectivity filter such as Glu-758 and Asp-1532 and reduce binding of TTX indirectly [37]. TTX-sensitivity of the channel is also affected by changes in membrane potential; toxin binding increases following repeated depolarizing pulses which increase availability of the TTX binding site [76, 77].

2.3 Adaptive evolution of elevated resistance to TTX in Na_V

There are several advantages for organisms to carry TTX. The toxin offers an excellent defence mechanism against potential predators. Puffer fish, for example, have no known predators other than humans [78]. TTX has been shown to function as a male-attracting pheromone at the time of spawning. Study of the puffer fish *Fugu niphobles* has shown that increased levels of TTX in ovulated oocytes releases TTX via the vitelline membrane and attracts males, but not females, to the spawning grounds, thereby increasing the chances of fertilization [79]. Conversely, TTX-resistance enables organisms to selectively feed on tetrodotoxic organisms. Some populations of the garter snake *Thamnophis sirtalis* feed on tetrodotoxic newts of the genus *Taricha* [80]. Studying the adaptive evolution of TTX-resistance in various organisms has provided an avenue to determine what changes are possible in highly conserved

portions of the Na_V. Cloning and sequencing of the cDNA of TTX-resistant channels has allowed us to observe what adaptive molecular changes have occurred in these channels. Studies have revealed that elevated resistance to TTX is due to point and multiple-site mutations in the pore region of Na_V [8-13].

2.3.1 TTX resistance in puffer fish

It is well known that puffer fish generally carry a high concentration of TTX without any adverse effects. Puffers contain TTX mainly on skin and in some internal organs, especially liver and gonads. The toxicity of puffer fishes varies among different species and depends on various factors such as seasonal, individual, and local variations [7]. It is proposed that TTX-resistance channels first arose in the Na_V of an early tetrodontid ancestor before diversification of the Tetraodontidae [12]. Yotsu-Yamashita and co-workers reported the genetic basis of TTX-resistant *Fugu paradalis* arises from the substitution of the non-aromatic amino acid Asn for an aromatic amino acid (Tyr or Phe) at 401 in the DI P-loop of Na_V 1.4a [9]. This site of mutation was also found in the Na_V1.4a of *Takifugu rubripes, Tetraodon nigroviridis,* and *Arothron nigropunctatus* and in four different genes of puffer fish sodium channels (Na_V 1.1a , Na_V 1.5a, Na_V 1.5b, and Na_V 1.6b) [7, 10]. This substitution of aromatic amino acid to non-aromatic amino acid at DI causes up to a 3,000-fold increase in resistance to TTX binding. Differential TTX-resistance might be determined by the side chain length in the non-aromatic amino acid residue. In addition to the substitution, replacement of Thr-759-Ser (or Asn) was reported in Na_V1.4a of *Arothron nigropunctatus* and *Tetraodon nigroviridis* and Na_V1.6b of *Canthigaster solandri* [12]. Mutation at Thr-759 might

induce a regional allosteric effect on Glu-758, a residue forming the outer ring, which could produce additional TTX-resistance from 2-fold up to 2,000 fold [75]. Mutation at Glu-758-Asp was reported in the Na_V 1.4b of *Tetradon nigroviridis* [10]. Various other amino acid substitutions in the pore region that confer TTX-resistance have also been reported in different species of puffer fish, including Met-1240-Thr in DIII, and Ala-1529-Gly, Ile-1561-Met, Asp-1568-Asn, and Gly-1569-Thr in DIV [12]. These findings are good examples of parallel evolution of TTX-resistance in puffer fish.

2.3.2 STX resistance in softshell clams

Saxitoxins (STX) are a family of water-soluble neurotoxins which also block sodium channels, and a similar mechanism of action has been proposed as for TTX [81]. STX selectively binds to the same amino acid residues in the outer pore loops of Na_V and occludes the channel pore. STX has a molecular skeleton structurally similar to TTX but with an additional positive guanidinium group and this structural difference of STX causes different binding affinities to Na_V [37, 46]. STX and its analogs are collectively called paralytic shellfish toxins (PST) and cause lethal paralytic shellfish poisoning (PSP). STX-producing dinoflagellates cause harmful algal blooms (red tides) and bivalve molluscs, which are the primary vectors of PSP in humans, exposed to such algal blooms accumulates PSP in their tissue [14]. Some populations of softshell clams, *Mya arenaria*, distributed in the Atlantic North America from the Gulf of St Lawrence to Chesapeake Bay, were found to carry STX, and amino acid sequence analysis reveals that STX-resistance derives from an amino acid substitution at Glu-758-

Asp in the DII of Na_V [14]. This substitution confers a 1,500-fold increase in STX-resistance and 3,000-fold increase in TTX-resistance [14]. This genetic adaptation to the harmful algal blooms permits increased survivorship of STX-resistant softshell clams, with reduced fitness of STX-sensitive individuals. Interestingly, identical DII Glu-758-Asp substitution was also observed in Na_V 1.4b of *Tetradon nigroviridis* [10]. These findings suggest sodium channels have the potential to develop neurotoxin resistance by single amino acid substitutions, and that substitutions in Na_V from completely different organisms result in the same molecular evolution under similar selective pressures.

2.3.3 TTX-resistance in garter snake

The garter snake, *Thamnophis sirtalis,* in the Pacific Northwest of the US is the only predator known to prey on the TTX-toxic newts *Taricha granylosa* which carry TTX concentrations in their skin sufficient to kill up to 25,000 white mice or seven humans [82]. TTX-resistance in the garter snake varies within populations, has a heritable basis and appears related to the level of toxicity and availability of the toxic newts [83-85]. In addition, the garter snake population dwelling in different geographical areas with the newts are not resistant to TTX, whereas co-localized ones are resistant [83].

Geffeney and co-workers studied four different garter snakes of the species *Thamnophis sirtalis* acquired from different geographical locations in the western United States: Bear Lake, Idaho; Warrenton and Benton County, Oregon; and Willow Creek, California [13, 86]. Three of these populations have co-evolved with the TTX-toxic newts *Taricha granulosa,* and phylogenetic

information indicates that their TTX-resistance has evolved independently (Figure 3) [80]. The phylogenetic relationships shown in Figure 3 were constructed based on mitochondrial DNA analysis of 19 western populations of *Thamnophis sirtalis* [80, 87]. Mitochondrial genes were extracted from genomic DNA and forward and reverse sequences for each gene were assembled. The g-test [87] and PAUP* [88] were employed to evaluate the phylogenetic content of the sequence and to conduct phylogenetic parsimony and maximum likelihood analyses. Garter snakes from outside of western population, Illinois and New York, were also sampled for comparison [80, 87].

TTX-resistance in these populations was observed by measuring the concentration of TTX required to block AP propagation in the skeletal muscle [86]. Garter snakes of Bear Lake, Idaho are the least TTX-resistance (1.0×10^{-7} M TTX), Warrenton and Benton, Idaho are intermediate in TTX-resistance (5.0×10^{-7} M TTX and 17.5×10^{-7} M TTX, respectively) and the most TTX-resistant Willow Creek snakes required 1.0×10^{-5} M TTX to block AP propagation. Similar to these findings, Brodie and co-workers reported that garter snake populations from California (Willow Creek, San Mateo, East Bay, and Omo) showed greatest organismic TTX-resistance, individuals from Oregon showed intermediate TTX-resistance (Warrenton, Benton, and Tenmile) and Idaho had had the least TTX-resistant garter snake populations (Bear Lake, Latah, and Selway) that they are TTX-sensitive [80]. These findings confirmed geographic differentiation in resistance to TTX within species.

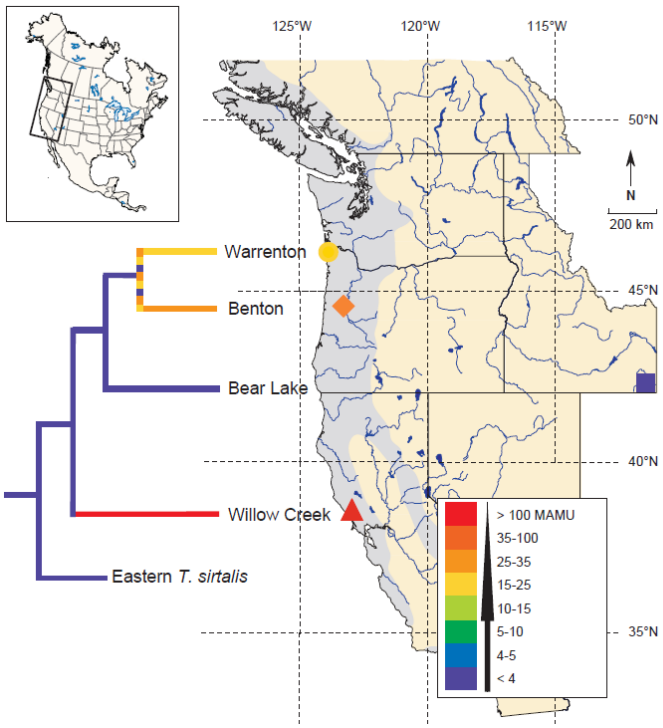

Figure 3. Localities and relationships of *Thamnophis sirtalis*.

Gray shaded region indicates range of newts of the genus *Taricha*. Colors correspond to level of whole-animal TTX resistance; legend includes all levels of resistance observed throughout western North America. Phylogeographic relationships and resistance evolution for these four populations are based on mitochondrial DNA analysis of 19 western populations of *T. sirtalis*. MAMU, mass adjusted mouse units. (This figure was taken from Geffeney *et al.,* 2002)

Mutations of genes that encode tsNa$_V$ 1.4 of garter snakes underlie TTX-resistance. The functional expression of tsNa$_V$1.4 revealed that the resistance to TTX was a consequence of substitutions of several amino acids in the DIV pore region (Figure 4) [13]. Warrenton, Benton, and Willow Creek populations shared amino acid substitution in which isoleucine is replaced by valine at 1561 in DIV [13]. The substitution occurs within the pore helix and may consequently alter the pore structure, thereby interrupting TTX binding affinity. This common

substitution in geographically isolated populations within the same snake species might represent parallel evolution. Sodium channels in the Benton County populations have an additional substitution at Gly-1566-Ala, and tsNa_V1.4 of Willow Creek garter snake possesses two more substitutions, Asp-1568-Asn and Gly-1569-Val. These additional mutations are proportional to organismic, action potential, and channel TTX-resistance [13, 86]. How the substitutions affect TTX binding is unknown. Similar patterns were observed in puffer fish Na_V1.4, including *Takifugu rubripes, Tetraodon nigroviridis*, and *Canthigaster solandri*. Additional mutations at the homologous Gly-1569 were observed to contribute significant TTX-resistance [9-13]. These findings suggest multiple amino acid substitutions impart greater neurotoxin resistance in sodium channels, and that similar substitutions occur in widely divergent organisms.

The geographic, expression, and mutational differences between TTX-resistant garter snake populations could result from differences in availability of the nontoxic prey and/or TTX content on the skin of the toxic prey [84]. Although an increased number of amino acid substitutions that cause greater TTX-resistance in the garter snake populations are beneficial for their fitness for preying on toxic newts, the substitutions may also cause negative impacts on survival, since more resistant snakes have a slower maximum run speed [89]. Run speed is determined, at least in part, by the influx of sodium ions through Na_V1.4 that generates and propagates APs in skeletal muscle. It has been reported that TTX-resistant Na_V isoforms tend to have lower conductance, slower kinetics and a more positive current-voltage relationship than TTX-sensitive

isoforms [61]. These data suggest the amino acid substitutions in TTX-resistant snakes may have biophysical sequelae resulting in slower maximum run speeds. A more complete assessment of how amino acid substitutions differentially affect the selectivity, permeability, and gating of the channel is required. Interestingly, substitutions found in the most TTX-resistant Willow Creek populations of garter snake, Ile-1561-Val and Asp-1568-Asn, were also observed in the DIV of T-type Ca^{2+} 3.3 channel, and permitted TTX to directly interact with the channel, blocking ion permeation [90].

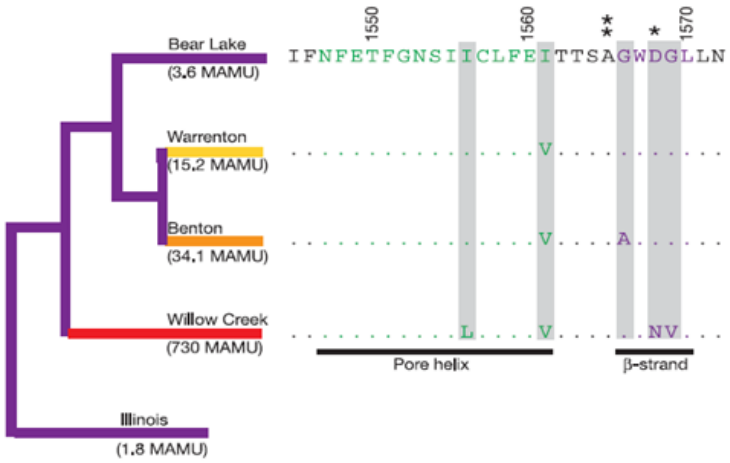

Figure 4. Amino acid sequence differences of four snake populations.

a, Phylogeographic relationships based on mtDNA analysis of 19 populations of garter snakes illustrate that separate origins of elevated TTX resistance for Willow Creek compared to Benton and Warrenton populations. Bear Lake is from a third lineage and is TTX-sensitive. Average whole animal TTX-resistance is shown in mass-adjusted mouse units (MAMU).

b, Amino acid alignment of part of the domain IV S5-S6 linker that affects TTX binding from tsNaV1.4. Selectivity filter (**) and outer charged ring (*) amino acids are labeled. The outer vestibule structure is stabilized by interactions between the pore helix and β-strand. Amino acids of the β-strand line the outer vestibule. (Figure from Geffeney et al., 2005)

3: MATERIALS AND METHODS

3.1 cDNA and mRNA Preparation

Human $Na_V1.4$ ($hNa_V 1.4$) α-subunit in SP64T was used as wild type (Bear Lake, BL, WT) since there is 100% sequence homology between hNaV1.4 and BL tsNaV1.4 in the DIV pore region [91, 92]. Rat Na_V 1.4 ($rNa_V1.4$) also contain 100% sequence homology and amino acid substitutions previously found in Warrenton and Willow Creek NaVs were inserted into $rNa_V1.4$ α-subunit by site-directed mutagenesis using a polymerase chain reaction (PCR) [93]. PCR recipe and associated solution include: 40 ng of template, 1 µL of 15 pmol of forward and reverse primers, 1 µL dNTPs (10mM stock), 5 µL 10X buffer and 1 µL Stratagene PFU polymerase and ddH_2O was added to make a total volume of 50 µL. PCR cycling conditions include 2 minutes of 94 °C for denaturation, 1 minute of 57-59 °C for annealing and 21 min of 72 °C for extension. The $rNa_V1.4$ α-subunit cDNA was subcloned from pTopo into pBSTA plasmid templates. Rat β 1-subunit cDNA were in pGH19. Before *in vitro* transcription, cDNA was linearized with EcoRI and NotI, respectively, and β_1-subunit with HindIII. For each clone, 1 µg of linearized template was used to perform in vitro transcriptions using mMessage mMachine Kits (Ambion): T7 polymerase for α-subunit and T3 polymerase for β_1-subunit. RNA for injection was resuspended in nuclease free water (Ambion) or 1 mM Tris-Cl pH 6.5 (Fluka) at a concentration of ~1 µg/µl.

Before injection, equal volumes of α- and β1-subunit mRNA were diluted to 1:10 ratio in nuclease free water (Ambion) and mixed together.

3.2 Oocytes Preparation and Injection

Oocytes were surgically removed from adult *Xenopus laevis* females. The frog was examined before selection to check if there was any signs of recent surgery; if not it was scooped with a aquarium net and placed in a closed container carrying anesthetic solution with 0.8 % tricaine methanesulfonate (Aldrich) in H_2O with 4.5 mM 1,4-(2-hydroxyethely)-1-piperazineethanesulfonic acid (HEPES) to stabilize pH. The closed container is used to prevent the frog from jumping out of the container which will result in contact with dry surface which will damage their protective mucus layer. The frog was left in the container for 20 minutes or until a firm toe-pinch with hemostats produces no response. Then the frog was placed on the surgical field and a 10-15 mm incision was made through abdominal skin and muscle. Small forceps was used to reach into the incision and several clumps of oocytes were extracted. During the surgery, the frog skin was well hydrated with sterile distilled water applied every 5 minutes. The incision was closed with 3-4 sutures on each abdominal skin and muscle and the frog was rinsed in deionized water until it recovered from the anesthesia. Theca and follicles were enzymatically removed by gently agitating the oocytes on the tube rocker in tube containing a Ca^{2+}-free medium (in mM): NaCl 96, KCl 2, $MgCl_2$ 20, HEPES 5, pH 7.4, with 1 mg/ml type 1A collagenase (Sigma, St. Louis, MO) for ~ 1 hr (until they appear 80~90 % separated). Oocytes were rinsed in the Ca^{2+}-free medium 3-4 times and decanted into a large (100 mm)

Petri dish. Under the dissecting microscope, healthy stage V and VI oocytes were sorted and placed in Petri dish containing SOS^+ solution containing(in mM): NaCl 96, KCl 2, $CaCl_2$ 1.8, HEPES 5, Pyruvic acid 2.5, pH 7.4,with 1 % Horse serum and Gentamycin Sulfate 100 mg/l. The sorted oocytes were incubated at 19°C. After 24 hrs of incubation, oocytes in good conditions were sorted again and individually injected with 27.6 - 50.6 nL of mRNA (mixture of α- and β_1-subunits) using a Drummond automatic Nanoject injector (PA, USA) and then placed in sterile incubation media containing They were incubated at 19°C and sorted daily into fresh SOS^+ solution until electrophysiological recording after 2-14 days.

3.3 Electrophysiology

Cut-open voltage clamp (COVC) recordings were completed following Stefani & Bezanilla [94]. Briefly, oocytes were placed in a rectangular triple compartment. Three compartments include the top recording chamber, the middle guard chamber and the bottom chamber where current is injected intracellularly [94]. The chambers were initially filled with external solution containing (in mM): 96 NaCl, 4 KCl, 1 $MgCl_2$, 1.9 $CaCl_2$, and 5 HEPES, (pH 7.4). The bottom chamber was briefly perfused with 0.1% saponin (Sigma) intracellular solution containing (in mM) 9.6 NaCl, 88 KCl, 11 EGTA, and 5 HEPES, (pH 7.4). Saponin-free intracellular solution was perfused upon perforation of the oocyte membrane. Recording electrodes were prepared using a P-87 micropipette puller (Sutter Instrument Co., Chicago, IL) with borosilicate glass to resistance

between 0.3 ~ 1.0 MΩ. Oocytes were impaled at the animal pole using recording electrodes filled with 3 M KCl. Temperature of the bottom chamber was measured and maintained at 20 ± 0.2 °C using a Peltier device controlled by an TC-10 temperature controller (Dagan, Minneapolis, MN, USA). Agar bridges made from glass capillary tubes with platinum wires filled with 3% agar in 500 mM NMG-MES were bent at both ends and placed in the three chambers and 1 M NaCl pools. Chloride silver wires in the NaCl pools connected agar bridges to a Dagan CA-1B amplifier (Dagan, Minneapolis, MN, USA). The sample interval was 5 μs (200 KHz) and data were low pass Bessel filtered at 10 KHz. Patchmaster v2X41 (Heka, Lambrecht, Germany) running on iMac computer (Apple, CA, USA) was used for data collection.

The holding potential for gating experiments was -100 mV. Activation kinetics were measured from the rising phase of inward current during 20 ms test depolarizations from a holding potential of –150 mV to voltages ranging from –100 mV to +60 mV. The voltage dependence of fast inactivation was studied with the following protocol: cells were held at -150 mV for 500 ms to remove all channels from inactivated states, then stepped to an alternating conditioning pulse between -150 mV and +20 mV in 10 mV increments, then to -10 mV for 20 ms then back to -150 mV. Peak inward current at -10 mV was measured and plotted versus conditioning pulse. Leak subtraction was performed using p/4.

Steady-state slow inactivation data was collected as follows. A 30 s, –150 mV prepulse was used to eliminate both fast and slow inactivation, and alternating conditioning 60 s pulses from –150 mV to +10 mV (in 10 mV

increments) were applied to induce maximal slow inactivation. A 20 ms recovery pulse to -150 mV is delivered to recover any fast inactivated channels followed by a 20 ms, 0 mV test pulse. Peak current amplitudes were normalized and plotted versus conditioning pulse.

Electrophysiological recordings of the sodium current were fitted into equations of interest described as below. Conductance (voltage) relationships were derived using the following equation:

$$G_{Na} = I_{peak} / (V_M - E_{Na}) \quad (1)$$

where G_{Na} represents sodium conductance, Imax is the peak-test-pulse current, V_M is the test-pulse voltage or pre-pulse voltage, and E_{Na} is the measured sodium equilibrium potential. Activation and inactivation curves are fitted by a Boltzmann distribution with the following equation:

$$\text{Normalized current amplitude} = 1/(1+\exp(-ze_0(V_M - V_{0.5})/kT)) \quad (2)$$

where 'Normalized current amplitude' was measured from the response to the test pulse following a variable voltage pre-pulse or from a holding potential of -150 mV, z is the apparent valence, e_0 is the elementary charge, $V_{0.5}$ is the midpoint voltage, k is the Boltzmann constant, and T is the temperature in degrees Kelvin.

The slow inactivation distribution was fitted by a modified Boltzmann equation as follows:

$$\text{Normalized current amplitude} = (1-f_a)/(1+\exp(-ze_0(V_M - V_{0.5})/kT)) + f_a \quad (3)$$

where z is the apparent valence, e_0 is the elementary charge, $V_{0.5}$ is the midpoint voltage, k is the Boltzmann constant, f_a is the fraction of the channel that did not enter slow inactivated state and T is the temperature in Kelvin.

To study whether mutations that resulted in TTX-resistance in mutant NaVs induce changes in ion selectivity, the COVC technique was used to measure sodium currents under different external solutions. Although two electrode voltage clamp (TEVC) is often used in studying ion selectivity and permeability of sodium channel [95-97], one distinct advantage of using COVC is it allows control over both external and internal solutions while TEVC can only replace external solution. In addition, COVC can record very large sodium currents with excellent voltage control and time resolution. The reversal potentials of the different sodium channels were compared to determine whether amino acid substitutions within the pore of TTX-resistant snakes had an effect on channel ion selectivity. Reversal potentials were measured by performing activation pulse protocols as previously described and fitting the current-voltage relationship to a Boltzmann distribution using equation 2 or calculating by linear extrapolation of normalized peak current versus membrane voltage relationship. Ionic permeability ratios P_X/P_{Na} were calculated from changes in the reversal potential following cation substitutions in the external solution with either Na^+, Li^+, K^+, Rb^+, or Ca^{2+} external solution. The external solution was titrated to pH 7.4 and contained, in mM: 96 NaCl or osmotic equivalent of test cation, 4 KCl, 1 $MgCl_2$, 1.9 $CaCl_2$, and 5 HEPES (Table 3). [98]. The permeability ratio (P_X/P_{Na})

for test cation was calculated using a modified Goldman-Hodgkin-Katz equation [99]:

$$\text{Permeability ratio} = P_X/P_{Na} = [Na]_1/[X]_2 \times \exp^{(F\Delta V/RT)} \quad (3)$$

where $[Na]_1$ is the concentration of sodium ion in Na^+ solution, $[X]_2$ is the concentration of cation in its solution, ΔV is the change in reversal potentials (E_{Xrev}- E_{Narev}), F is Faraday's constant, R is the ideal gas constant, and T is the temperature in Kelvin.

3.4 Data Analysis

Analysis and graphing were done using FitMaster (Heka, Lambrecht, Germany) and Igor Pro (Wavemetrics, OR, USA), both run on Apple iMac (CA, USA). Results are expressed as mean ± standard errors of mean (SEM) and statistical significance was determined by ANOVA test with two tailed P-values ($P<0.05$) using a statistical analysis program, SPSS 17 (SPSS, IL, USA).

Table 3. Composition of external solutions.

	pH	NaCl (mM)	KCl (mM)	LiCl (mM)	RbCl (mM)	$CaCl_2$ (mM)	$MgCl_2$ (mM)	Hepes (mM)
Na^+	7.4	96	4	0	0	1.8	1	5
Li^+	7.4	0	4	96	0	1.8	1	5
K^+	7.4	0	100	0	0	1.8	1	5
Rb^+	7.4	0	4	0	96	1.8	1	5
Ca^{2+}	7.4	0	4	0	0	97.8	1	5

E_{rev} is reversal potential, $V_{0.5}$ is the voltage activation midpoint, *z* is apparent valence, and *n* is number of experiments. Values are 'mean±SEM'

4: RESULTS

4.1 Biophysical Properties of Channel Gating.

Sodium currents were recorded from *Xenopus oocytes*, expressing both α and β subunits, using the cut-open voltage clamp technique to test the hypothesis that amino acid substitutions, which impart TTX resistance in snake skeletal muscle sodium channels, result in changes in voltage dependent gating. I examined human and rat $Na_V1.4$ containing sequence from different garter snake populations, including Bear Lake, Idaho (BL); Warrenton, Oregon (WA); and Willow Creek, California (WC). To ensure β subunit was properly co-expressing with α subunit, data were first collected from oocytes expressing α subunit alone and compared to cells injected with both α and β subunits. As reported in previous studies, expression of β subunit altered kinetics of steady-state fast inactivation by causing significant right shift in $V_{0.5}$ of cells with β subunit whereas that of conductance was not affected (Figure 5 and Table 4) [15, 100]. In addition, co-expression of α and β subunits increased the number of apparent valence charges, the slope of fitted lines, in conductance (Figure 5 and Table 4). These data indicate that α and β subunits were appropriately co-expressing in oocytes as it is in the physiological setting.

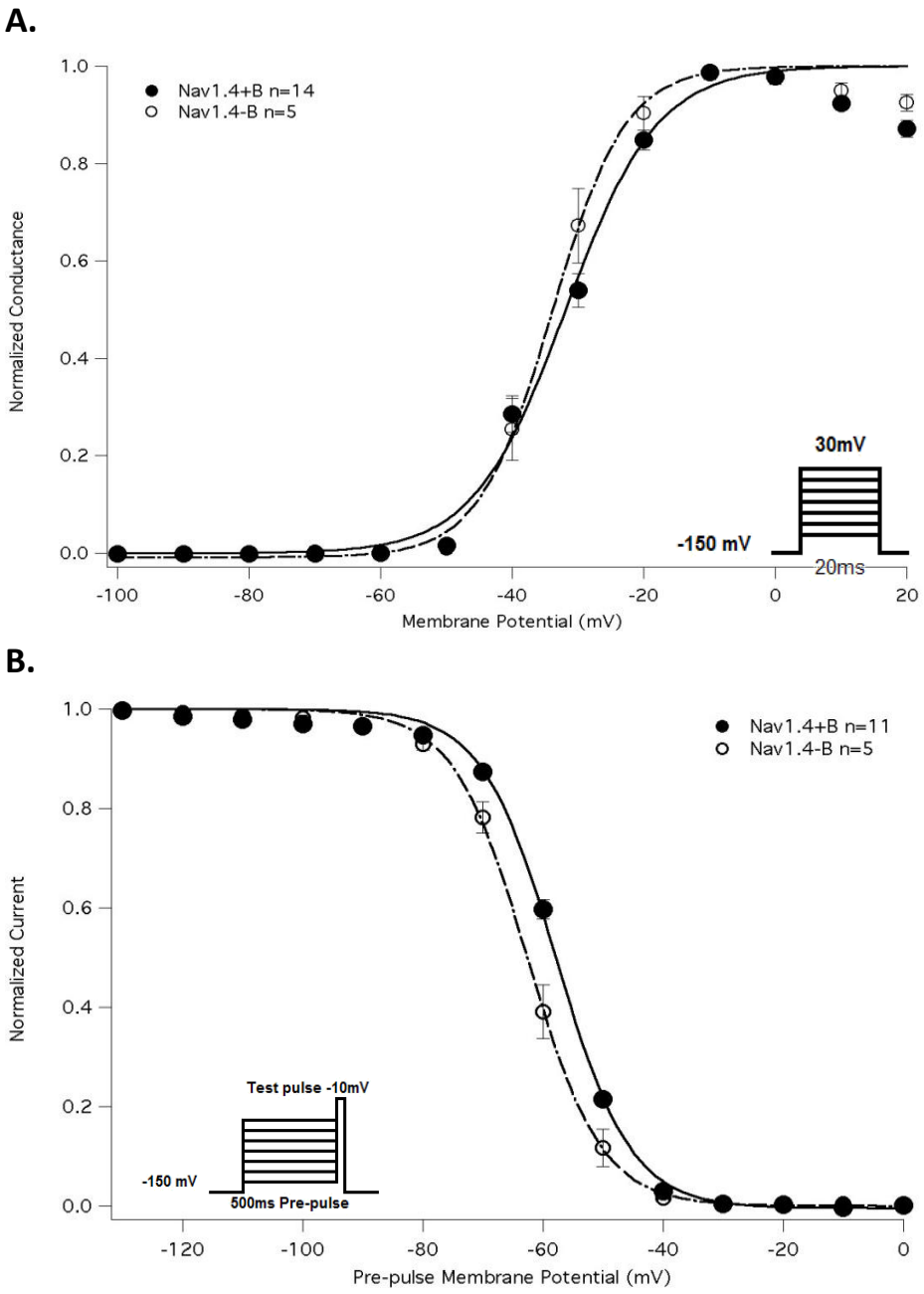

Figure 5. Gating Properties of Wild Type $Na_V1.4$ with or without β subunit.

A. Conductance graph of normalized mean peak currents (±SEM) versus membrane potential: Nav1.4 with β subunit (closed circles, *N*=14), and Nav1.4 without β subunit (open circles, *N*=5). Protocol used is illustrated as above.

B. Effect of β subunit in Na_V 1.4 steady-state fast inactivation. Normalized mean peak currents (±SEM) versus pre-pulse membrane potential is shown in the graph: Nav1.4 with β subunit (closed circles, *N*=11), and Nav1.4 without β subunit (open circles, *N*=5). Protocol used is shown as above.

Table 4. Effect of Summary of β subunit in $Na_V1.4$ gating properties.

	E_{rev} (mV)	GV $V_{0.5}$ (mV)	GV slope	FI $V_{0.5}$ (mV)	FI slope
Nav1.4	**50.7 ± 3.6(5)**	**-33.8 ± 1.8(5)**	**5.37 ± 0.55*(5)**	**-62.5 ± 1.4 (5)**	**-4.32 ± 0.24(5)**
Nav1.4+ β	**52.8 ± 1.9(14)**	**-31.5 ± 1.1(14)**	**3.91 ± 0.21(14)**	**-57.7 ± 0.3 (11)**	**-4.09 ± 0.11(11)**

* denotes statistical significance ($p<0.05$). GV is conductance, FI is fast inactivation, E_{rev} is reversal potential, $V_{0.5}$ is the voltage activation midpoint, slope is the slope of the fitted line which refers to apparent valence charges and numbers in parentheses indicate number of experiments. Values are 'mean±SEM'

4.1.1 Activation

A typical family of sodium currents from Bear Lake (BL), Warrenton (WA) and Willow Creek (WC) Na_V are illustrated in Figure 6. To assess the current-voltage relationship of the channels, the peak currents of each trace were measured and plotted against the test potential as shown in Figure 7. The voltage dependence of activation was further evaluated by plotting normalized macroscopic conductance as a function of the test potential, and fitted with the Boltzmann equation (Equation 2), as shown in Figure 8. Statistically significant hyperpolarizing (left) shifts of ~6 mV in V0.5, and significantly greater values in the slope were observed in WC compared to BL (Table 5).

Table 5. Biophysical parameters of the channel activation.

		E_{rev} (mV)	$V_{0.5}$ (mV)	Slope (*e*)	*n*
Bear Lake	Wild Type	**52.8 ± 1.9**	**-31.5 ± 1.1**	**3.91 ± 0.80**	**14**
Warrenton	I1532V	**46.1 ± 2.3***	**-32.6 ± 1.5**	**3.61 ± 0.49**	**11**
Willow Creek	I1527L/I1532V/ D1539N/G1540V	**44.9 ± 0.9***	**-37.3 ± 1.3***	**5.97 ± 0.77***	**18**

* denotes statistical significance ($p<0.05$) with respect to the values obtained from Bear Lake (WT). E_{rev} is reversal potential, $V_{0.5}$ is the voltage activation midpoint, slope is the apparent valence of conductance and *n* is number of experiments. Values are 'mean±SEM'

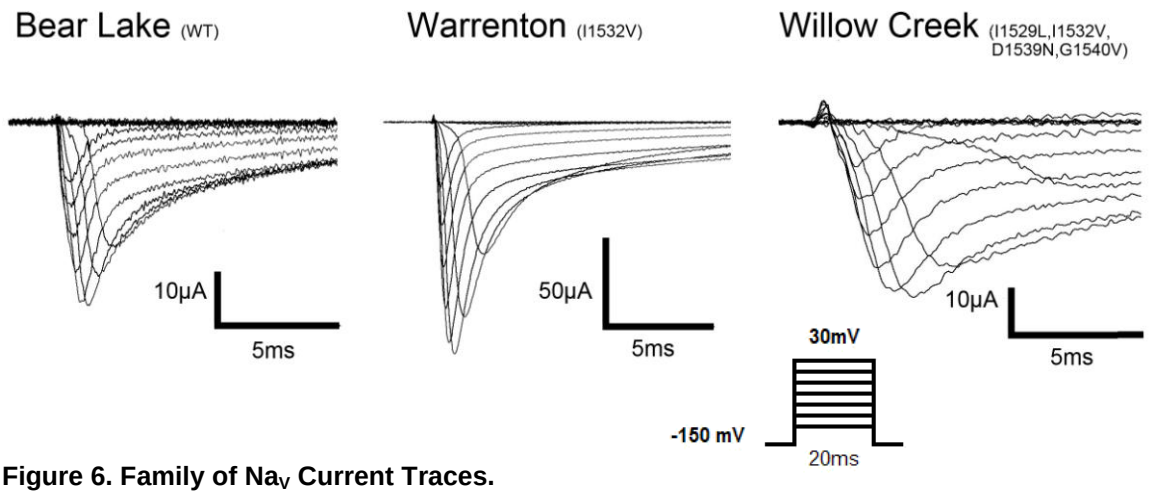

Figure 6. Family of Na_V Current Traces.

Family of sodium current traces were recorded using cut-open voltage clamp from *Xenopus* oocytes. Holding membrane potential was at -100 mV and prior to test voltage, membrane was hyperpolarized to -150 mV for 500 ms to ensure complete shutdown of the channel. Pulse protocol is depicted as above.

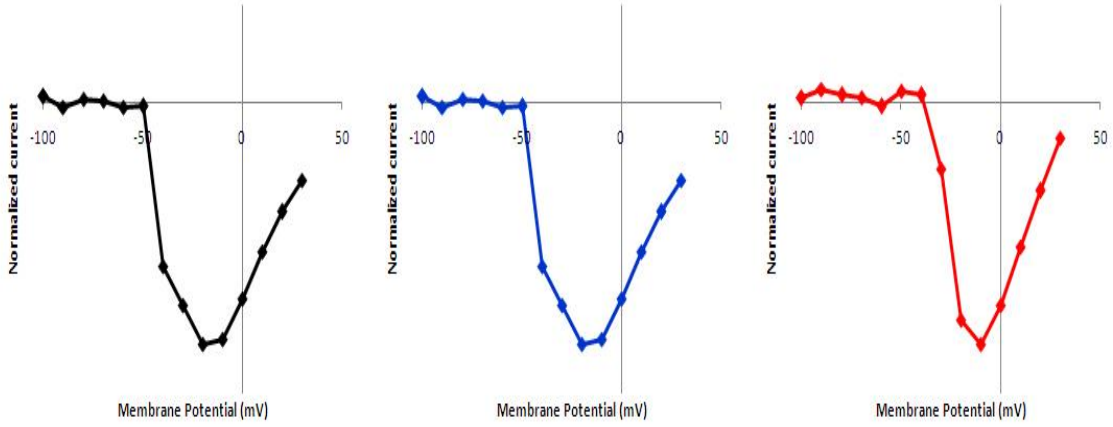

Figure 7. Peak Na_V current vs. Voltage Graphs.

Peak currents from Figure 6 were plotted against membrane potential to demonstrate voltage dependence of the channels.

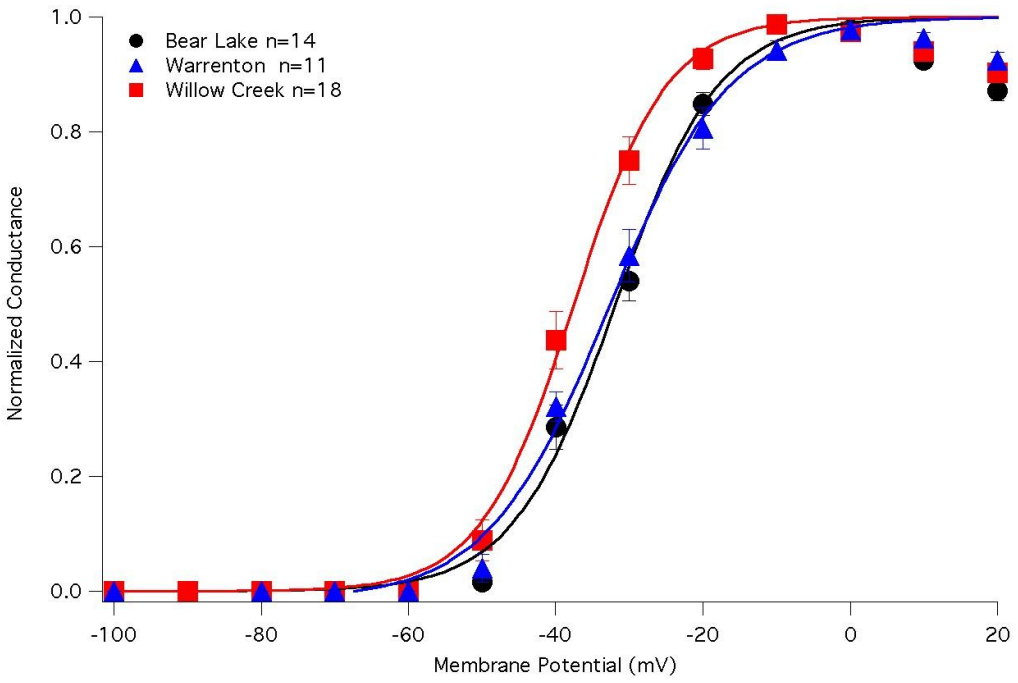

Figure 8. Activation of sodium channels.

A graph of mean normalized conductance (±SEM) versus membrane potential: *Bear Lake* (black circles, *N*=14), *Warrenton* (blue triangles, *N*=11), and Willow Creek (red squares, *N*=18).).

4.1.2 Fast Inactivation

To measure steady-state properties of fast inactivation, cells were held at -150 mV and 500 ms of alternating pre-pulse potentials ranged from -150 mV to -10 mV in 10 mV steps were applied. The cell was then depolarized to the test voltage of 0 mV, and peak inward current was recorded, normalized and plotted against pre-pulse membrane potential as shown in Figure 10. A depolarizing shift in the midpoint of steady-state fast inactivation was seen in both TTX-resistant channels compared to the TTX-sensitive channel, and the apparent valence was decreased (Table 6).

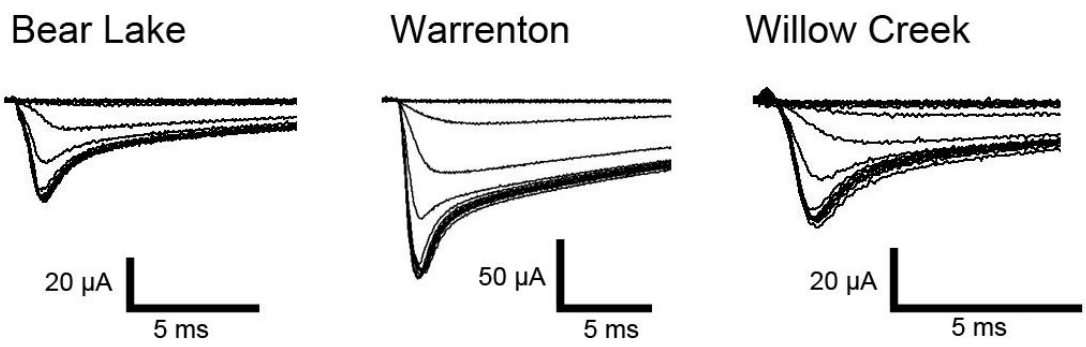

Figure 9. Steady-State Fast inactivation raw current traces

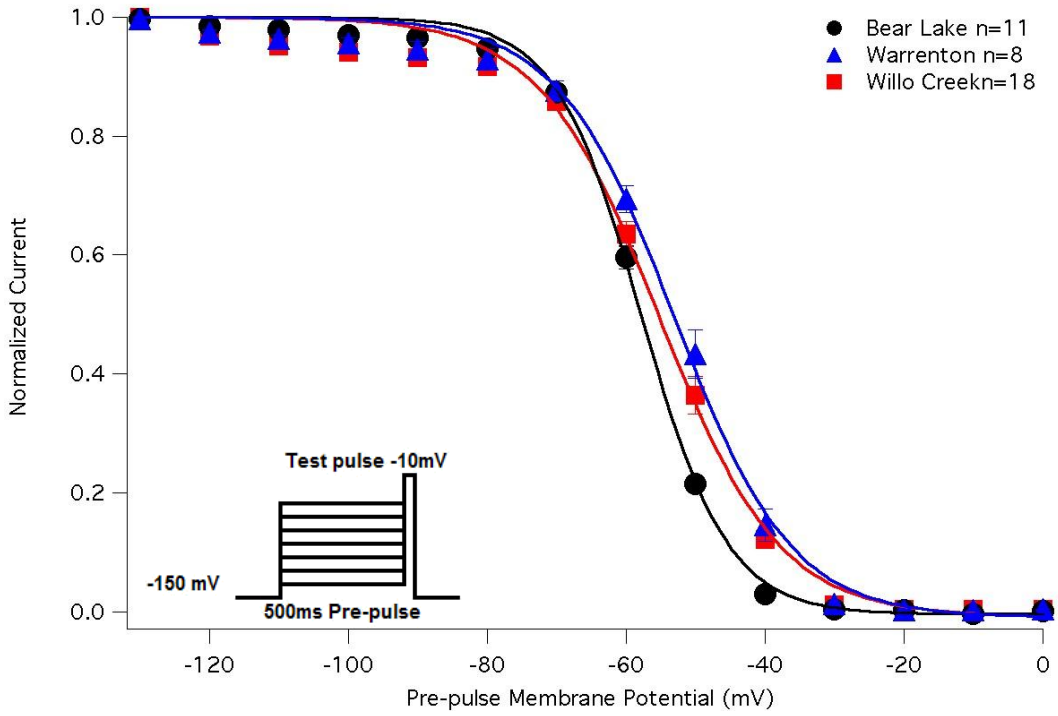

Figure 10. Steady-State Fast Inactivation of sodium channels.

A graph of steady-state fast inactivation illustrates the channel availability after 500 ms pre-pulses to various voltages ranging from -150 mV to -10 mV. Mean normalized current (±SEM) versus pre-pulse membrane potential were plotted: *Bear Lake* (black circles, *N*=11), *Warrenton* (blue triangles, *N*=8), and Willow Creek (red squares, *N*=18).

Table 6. Biophysical parameters of steady-state fast inactivation of the channels

	$V_{0.5}$ (mV)	Slope (*e*)	*n*
Bear Lake	**-57.7± 0.3**	**-4.09 ± 0.11**	**11**
Warrenton	**-53.3.3 ±0.2***	**-3.22 ± 0.15***	**8**
Willow Creek	**-55.5 ± 0.7***	**-3.25 ± 0.16***	**18**

$V_{0.5}$ is the voltage when normalized current is 0.5, slope is the apparent valence of inactivation and *n* is number of experiments. Values are given as 'mean±SEM'

4.1.3 Slow Inactivation

Steady-state slow inactivation (SI) was measured using a voltage pulse protocol identical to steady-state fast inactivation except the alternating pre-pulse potential was 60s in duration and there was a 20ms hyperpolarization to-150 mV following the pre-pulse to recover channels from fast inactivation. The test potential was 0mV. Between protocols, channels were hyperpolarized to -150 mV for 30s after each trial to prevent accumulation of SI [101]. The steady-state SI distribution was fitted with a modified Boltzmann equation (Equation 3), which takes into account the incomplete nature of slow inactivation at depolarized voltages. The midpoint of steady-state SI in the TTX-resistant channels was significantly depolarized relative to the TTX-sensitive channel (Figure 12 and Table 7).

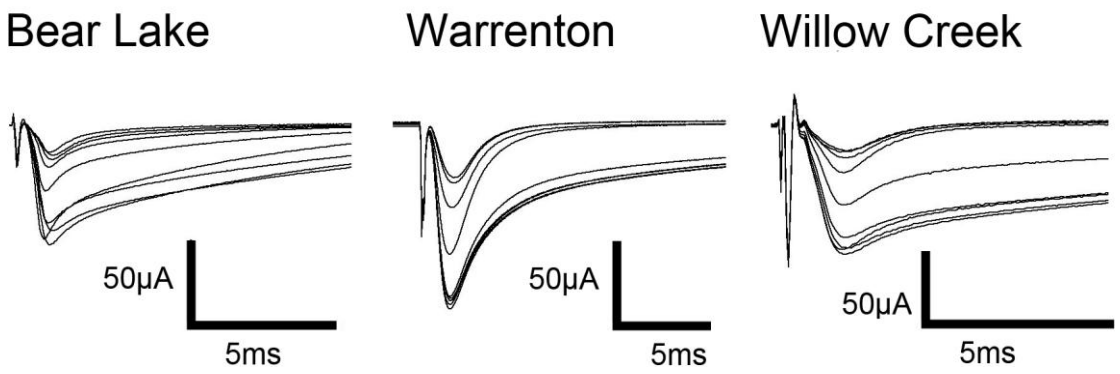

Figure 11. Steady-State Slow inactivation raw current traces

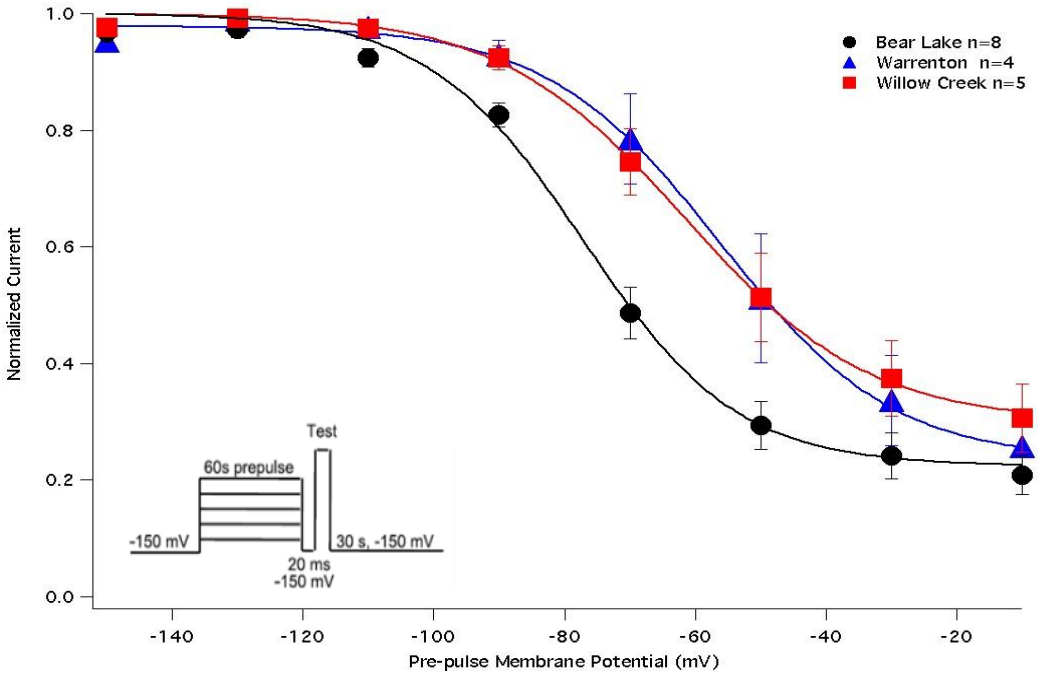

Figure 12. Steady-State Slow Inactivation of sodium channels.

A graph of steady-state slow inactivation illustrates the channel availability after 60 s pre-pulses to various voltages ranging from -150 mV to -10 mV. Mean normalized current (±SEM) versus pre-pulse membrane potential were plotted: *Bear Lake* (circles, *N*=8), *Warrenton* (triangles, *N*=4), and Willow Creek (squares, *N*=5).

Table 7. Biophysical parameters of steady-state slow inactivation of the channels.

	$V_{0.5}$ (mV)	Slope	Completion	*n*
Bear Lake	-76.0 ± 1.7	-2.15 ± 0.33	80.2 ± 3.3%	8
Warrenton	-56.4 ± 6.0*****	-2.04 ± 0.22	77.0 ± 5.3%	4
Willow Creek	-60.4 ± 3.5*****	-1.84 ± 0.09	70.6 ± 5.4%	5

$V_{0.5}$ is the voltage when normalized current is 0.5, slope is the apparent valence of inactivation, completion is the percentage of channel available at the most positive pre-pulse membrane potential and *n* is number of experiments. * denotes statistical significance ($p<0.05$) with respect to the values obtained from Bear Lake (WT). Values are given as 'mean±SEM'

4.2 Ion Selectivity of Channel

Ion selectivity in Na_V can be studied by observing the voltages at which the ion currents reverse their direction [95, 97]. The reversal potential (E_{rev}) in different sodium channels were compared to determine whether substitutions imparting TTX-resistance altered ion selectivity. The E_{rev} of BL was 52.8 mV (± 1.9 mV). In contrast, WA was 46.1 mV (± 2.3 mV)and WC was 44.9 mV (± 0.9 mV). These differences were statistically significant, and suggest that the ion selectivity of the TTX-resistant channels is different from that of WT.

We measured and compared the permeability ratio of channels by measuring currents under different external solutions including the following permeant ions: Li^+, K^+, Rb^+ and Ca^{2+} To ensure a constant electrochemical gradient across the cell membrane and to avoid any ion build-up in the

cytoplasm, the internal solution was also continuously perfused with the internal solution. A typical family of sodium currents of sodium channels under Li^+ external solution is illustrated in Figure 13. Figure 14 shows the mean normalized current (±SEM) as a function membrane potential for the different external permeant ions. The TTX-sensitive wild type, BL, exhibited permeability ratios of 1.44 (± 0.19) for Li^+, 0.20 (± 0.03) for K^+, 0.17 (± 0.03) for Rb^+ and 0.37 (± 0.06) for Ca^{2+}. The mildly TTX-resistant channel, WA, displayed permeability ratios that were not significantly different from BL (Table 8).

Interestingly, the highly TTX-resistant channel, WC, showed a significant decrease in permeability ratios: 0.88 (± 0.05) for Li^+, 0.11 (± 0.02) for K^+, 0.09 (± 0.01) for Rb^+ and 0.16 (± 0.02) for Ca^{2+} (Table 8). Permeability ratio values as a function ionic radius, a measure of the size of an ion in a crystal lattice, are shown in Figure 15. Permeability ratio of the cations; the Pauling radius of cations are 0.60 Å for Li^+, 0.99 Å for Ca^{2+}, 1.33 Å for K^+, and 1.48 Å for Rb^+ [102]. Our results indicate that amino acid substitutions in the pore region of DIV affect the ion selectivity and permeability of Na_V.

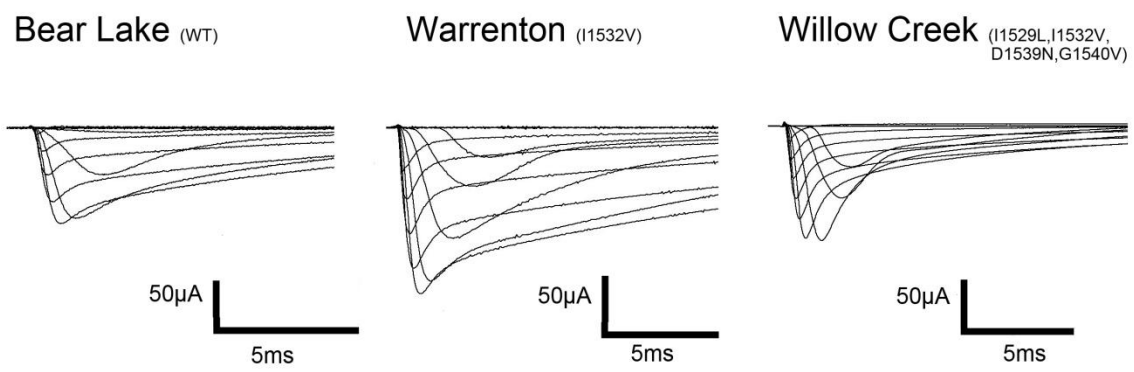

Figure 13. Family of current traces recorded using Li^+ external solution.

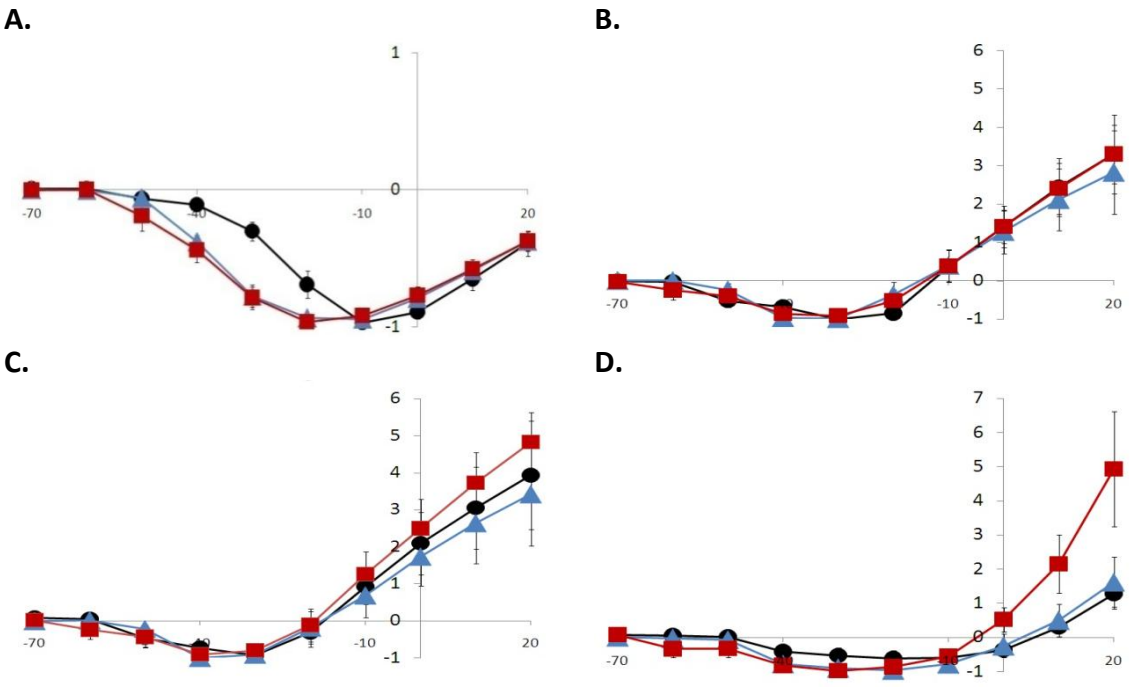

Figure 14. Normalized current and voltage relationship under different external solutions.

Mean normalized currents (±SEM) of *Bear Lake* (circle, *N*=4), *Warrenton* (triangle, *N*=4), and Willow Creek (square, *N*=4). Currents were normalized with the peak inward current. Normalized currents versus membrane potentials were plotted under different external solutions: **A.** Li^+, **B.** K^+, **C.** Rb^+, and **D.** Ca^+

Table 8. Summary of Reversal Potential and Permeability Ratio.

		Li^+	K^+	Rb^+	Ca^{2+}	*N*
Bear Lake	E_{rev} (mV)	38.0 ± 5.6	-10.8±2.1	-17.3±2.5	3.5±1.3	4
	P_X/P_{Na}	1.44 ± 0.19	0.20 ±0.03	0.17±0.03	0.37±0.06	
Warrenton	E_{rev} (mV)	40.9 ± 2.8	-10.7 ± 4.3	-12.9 ± 4.7	8.3 ± 4.7	4
	P_X/P_{Na}	1.10 ± 0.02	0.14 ± 0.01	0.13 ± 0.02	0.30 ± 0.02	
Willow Creek	E_{rev} (mV)	39.6 ± 1.7	-12.9 ± 3.8	-18.4 ± 3.4	-3.0 ± 2.8	4
	P_X/P_{Na}	0.88 ± 0.05*	0.11 ± 0.02*	0.09 ± 0.01	0.16 ± 0.02*	

* denotes statistical significance ($p<0.05$) with respect to the values obtained from Bear Lake (WT). E_{rev} is reversal potential, P_x/ P_{xNa} is the permeability ratio, and *n* is the number of samples. Values are given as mean±SEM

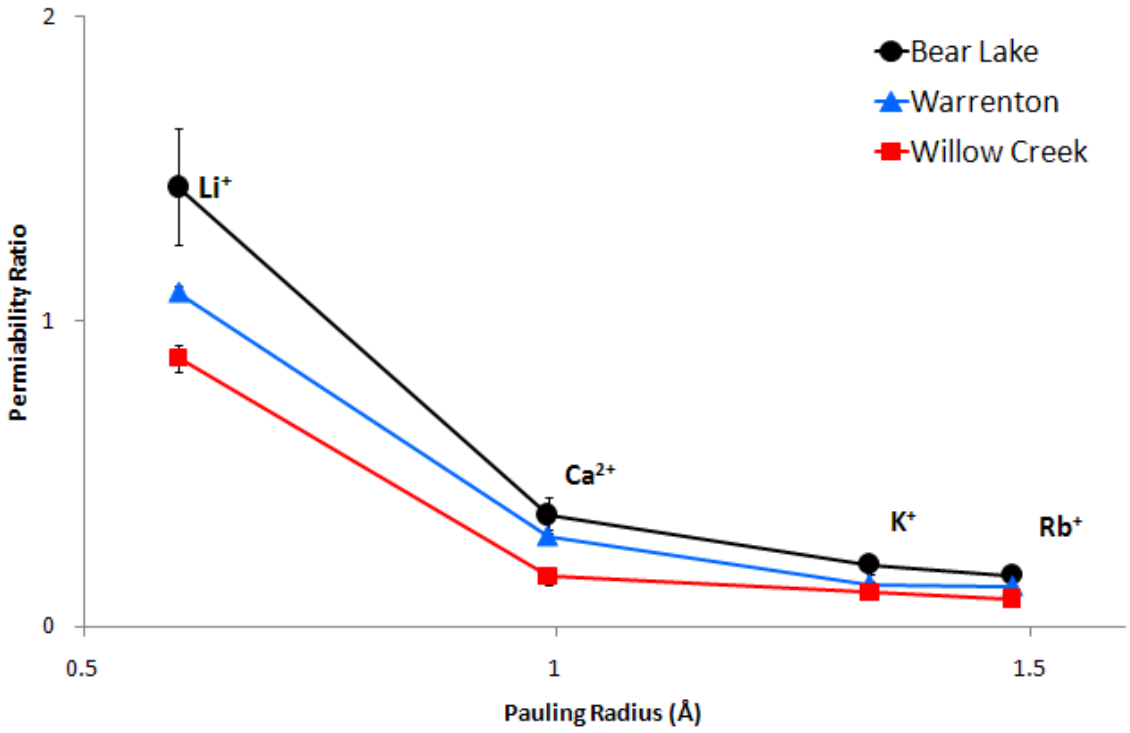

Figure 15. Permeability ratio of the cations

Mean permeability ratio (±SEM) of *Bear Lake* (circle, *N*=4), *Warrenton* (triangle, *N*=4), and Willow Creek (square, *N*=4). Pauling radius of cations are 0.60 Å for Li^+, 0.99 Å for Ca^{2+}, 1.33 Å for K^+, and 1.48 Å for Rb^+ [102].

5: DISCUSSION

The garter snake, *Thamnophis sirtalis,* is the only predator known to prey on the TTX-toxic newts *Taricha granulosa* which has enough TTX in their skin to kill up to 25,000 white mice or seven humans [82]. Toxicity in newts exerted selection pressure on its predator resulting in amino acid substitutions in the P-region of DIV skeletal sodium channel [13]. Toxicity in newts is closely related to the degree of TTX resistance in the garter snake as well as the number of amino acid substitutions in sodium channel. Although an increased number of amino acid substitutions that cause greater TTX-resistance in the garter snake are beneficial for their predator fitness, the substitutions may also cause negative impacts on survival, since more resistant snakes have a slower maximum run speed and slower AP rise rate [89]. Run speed and AP rise rate are determined, at least in part, by the influx of sodium ions through sodium channels that generate and propagate APs in skeletal muscle. Thus, mutations may have compromised the biophysical properties of Na_V. The goal of our study was to examine the effects of these amino acid substitutions on the gating properties and ion selectivity of Na_V.

In this study, we observed significant changes in the activation profile of the most TTX-resistant channel (WC) and inactivation profiles in both TTX-resistant channels, WA and WC. Many studies have shown the importance of the P-regions in channel function [35, 40, 41, 103, 104]. The pore forming P-region of

DIV is highly conserved in Na_V, and site-directed mutagenesis studies have shown that it is responsible for voltage-dependent activation [35] and inactivation [33, 105] as well as ion permeation and selectivity [95, 96]. Amino acid substitutions found in TTX-resistant garter snake Na_V are in a region near the selectivity filter between theα-helix and β-strand of the P-region, where the loop forms a sharp bend to stabilize the structure of the pore mouth [46]. In addition, an important negatively charged aspartate residue in the pore region of DIV that interacts with a hydroxyl group on TTX was neutralized through amino acid substitution with asparagines in WC [75]. These substitutions may have reduced TTX binding by altering the outer vestibule of the pore, and thus the shape of the TTX binding site. These changes in the outer vestibule of the pore may reorient the overall channel structure, thus disrupting the coupling between the voltage sensors and the ion permeation pathway of the channel, the movement of the ion permeation pathway, and reducing pore stability.

5.1 Effect on the Voltage Dependent Gating of Na_V

WC contains four amino acid substitutions that confer TTX binding affinity that is ~480 fold less than BL and ~270 fold less than WA [13]. The mutations, however, also significantly affected activation of WC. How do the mutations alter the activation profile of WC? Coupling between the pore and the voltage‐dependent movements of the voltage sensor units is an important determinant of channel opening in Na_V. The movements or reorientations of the positively charged S4 segments toward the extracellular side in response to depolarization lead to pore opening through several steps. Activation of the S4

voltage sensors in DI, DII and DIII which are kinetically indistinguishable initiates the channel opening [23]. The DIV S4, however, activates at a relatively slower rate and in a two-step process; the initial step involves movement of the internal segment and is critical for activation whereas the latter step, movement of the external segment, is required for inactivation [106]. Channel activation, therefore, requires full activation of the S4 segments in DI, DII, and DIII and a partial activation of the S4 of DIV [106-108]. Full activation of the S4 of DIV uncovers the intracellular binding site for the inactivation particle and subsequently allows the channel to enter the fast inactivated state [23, 24, 106, 107]. In addition, DIVS4 plays important role in slow inactivation [109]. Therefore, changes in the voltage-dependent movements of any of the S4 voltage sensors may be reasonably predicted to Na_V alter gating. In this study, we observed significant changes in the activation profile of WC Na_V and inactivation profiles in both mutant Na_Vs. These changes suggest that amino acid substitutions in the P-region of DIV may have altered the interaction between the voltage-dependent movements of any of the S4 voltage sensors and the P-region. It is tempting to speculate that the reorientation of the pore might even result in a channel structure that physically hinders movement of the one or more of the S4 voltage sensors.

The substitutions in WC include charge neutralization at the outer ring residue of DIV, aspartate at 1539 replaced by asparagine, and a change in the net charge of the outer ring may have caused altered activation of the channel. This charge neutralization, however, was previously studied and shown to have

no effect on the voltage dependence of activation [103, 110]. Khan and coworkers [110] proposed that the distance between the outer vestibule residues and the voltage sensor units responsible for voltage dependence of activation may be far apart and the electric field of the outer vestibule is likely dispersed by the surrounding extracellular ionic solution causing no effect on activation when the charge was neutralized. Interestingly, when aspartate at 1539 was replaced with cysteine, a significant decrease in conductance was observed [111]. This may be due to a size difference between aspartate and cysteine that may cause changes in the pore structure, since the structurally-conservative D1539N mutation did not alter activation. Nonetheless, charge neutralization in the selectivity filter can electrostatically destabilize and/or weaken the interaction between the P-region of DIV with the P-regions in DI and DIII [112]. This can subsequently lead to changes in the structure of the ion permeation pathway that may reduce pore stability [105].

A number of studies have established that the P-regions of Na_V are highly flexible structures [112-114]. It is proposed that, at rest, the pore forming P-regions fold back into the pore lumen surrounded by the S6 segments and undergo some kind of movement during channel opening [41, 45]. Any interference with this motion may result in altered channel gating. Two glycine residues in the P-region of DIV (G1537 and G1540) confer a high degree of backbone flexibility and are associated with the movement resulting in a conformational change during channel activation. In WC, glycine at 1540 is substituted by valine, and this may cause the altered activation profile observed

in our experiment by reducing the flexibility of the channel backbone and disrupting pore movement during channel opening.[115].

Another amino acid replacement, leucine substituted for isoleucine at position 1527, is located within an α-helical region of the P-region [46]. The α-helix structure is composed of highly hydrophobic residues and its hydrophobic characteristic is well conserved since leucine is non-polar hydrophobic residue. This suggests that the α-helix structure is important in maintaining the pore structure and its proper function. However, how this mutation would affect the TTX binding to the pore is not clear and further study is required. This mutation may provide an additive effect in WC that both imparted greater TTX-resistance and modified the voltage-dependence of activation.

WA contains a single mutation that confers a TTX-binding affinity ~2 fold less than BL. In contrast to WC, the single residue substitution in WA that is also observed in WC did not affect channel activation. However, the substitution, isoleucine to valine at position 1532, altered both fast and slow inactivation. Previous studies have shown that mutations in P-regions of Na_V alter the properties of slow inactivation but not fast inactivation [45, 116]. Although the differences in fast inactivation profiles between WT and mutant channels were statistically significant, they were quantitatively small (Table 6), suggesting that the difference between our results and previous studies may be due to a difference between human Na_V and rat Na_V gating. Nonetheless, we cannot rule out the fact that amino acid substitutions in WA and WC channels may have indirectly affected fast inactivation through a change in overall channel structure,

since previous studies have shown, under the same experimental conditions, activation and steady-state fast inactivation of human Na_V and rat Na_V are statistically similar [26, 117].

Slow inactivation of both WA and WC showed significant depolarizing shifts of ~20 mV in midpoint relative to WT

(

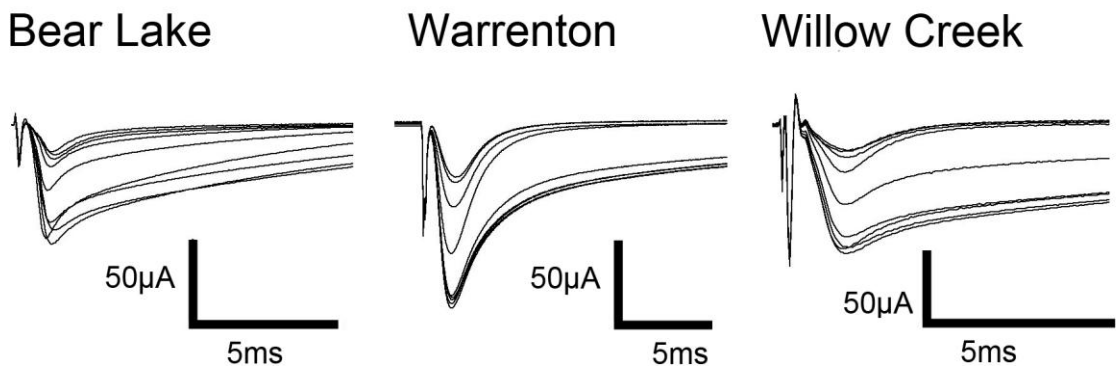

Figure 11. Steady-State Slow inactivation raw current traces

). This result suggests an increase in the number of channels available to open during a depolarizing step and thus, cell excitability is greater in TTX-resistant channels than WT. However, the maximum probability of channels entering slow inactivated state did not differ from WT

(

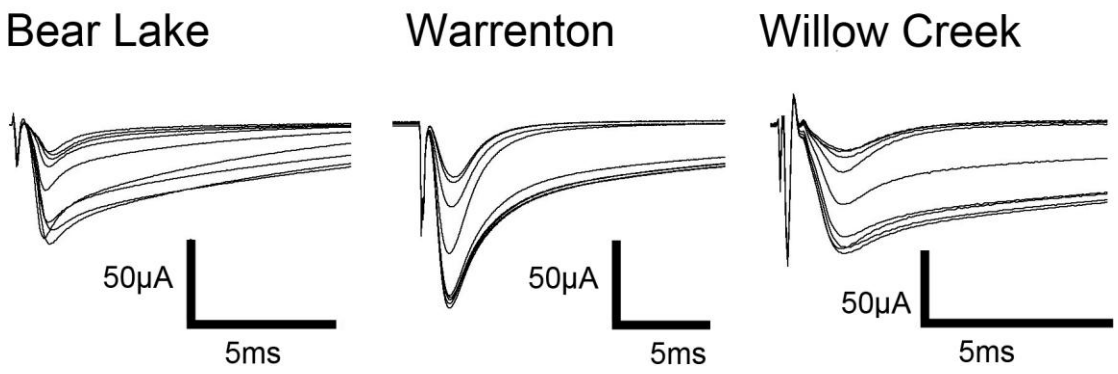

Figure 11. Steady-State Slow inactivation raw current traces

). The depolarizing shifts were statistically similar in both TTX-resistant channels suggesting altered slow inactivation may arise from the same substitution. Therefore, we suggest that isoleucine at position 1532 may play important role in steady-state slow inactivation of Na_V.

It has been proposed that slow inactivation in Na_V arises from a constriction or collapse of the ion permeation pathway and that residues within or proximal to selectivity filter are closely related to the conformation change during slow inactivation [30, 31, 33, 45]. In *Shaker* K^+ channels, C-type (slow) inactivation is also associated with pore constriction related to structural rearrangements in the P-regions. In addition C-type inactivation is closely related to the gating motion of voltage sensors [29] and I1532L may have altered the movement of the voltage sensor disrupting the coupling between the pore and the voltage sensors causing change in slow inactivation profile in mutant Na_Vs.

Depolarization of the channel activates the voltage sensor to enter its depolarization-favored position [108]. During prolonged or repeated depolarizations of the channel, we envision the voltage sensors to go through a secondary transition from its depolarization-favored position which changes the way in which the voltage sensor interacts with the pore region and consequently alters the conformation of the ion permeation pathway. Since DIV S4 plays an important role in both fast and slow inactivation, it is likely that this segment is affected by the I1532L. This hypothesis, however, needs to be experimentally confirmed.

Recent work from Yang *et al.* showed the DIV P-region interacts with DIV S6 and serves an essential role in coordinating channel gating and ion permeation [116]. Changes within the DIV P-region structure may also affect the interaction with the adjacent DIV S6, which plays an important role in fast and slow inactivation [32, 118, 119]. DIV S6 is in close contact with the DIV P-region. Allosteric changes due to the I1532L substitution may be transferred to DIV S6 and thus alter inactivation properties [114]. It is possible that the I1532L substitution in both WA and WC alter slow inactivation by interrupting the interaction between the P-region and DIV S6.

5.2 Effect on the Ion selectivity and Permeability of Na_V

The ion selectivity filter is very complex; it interacts with, and filters, inorganic ions based on various factors including their size, charge, and

dehydration energy. Site-directed mutagenesis studies have demonstrated that mutations of amino acid residues within or proximal to the DIV selectivity filter modify selectivity [11, 12, 35, 38, 95, 96]. For instance, mutation of the negatively charged residues that forms the outer ring of the channel selectivity filter in DIV significantly altered ion selectivity and permeability of Na_V [95]. Ion selectivity in Na_V can be studied by observing the voltages at which the ion currents reverse their direction (E_{rev}). Our results revealed that E_{rev} of TTX-resistant Na_V significantly differed from WT; E_{rev} was shifted toward more negative voltages, indicating the amino acid substitutions have altered the ion selectivity of TTX-resistant channels.

We used Li^+, K^+, Rb^+ and Ca^{2+} external solutions to observe permeability of the channel by these ions. These cations were chosen because their permeability ratios have been previously studied in WT channels, and mutations of the selectivity filter residues have shown to alter their permeation [95, 96, 98]. Our results showed that the permeability ratios of WA did not statistically differ from those of WT Na_V. WC permeability ratios, however, were significantly lower than WT (Table 8). Negatively charged amino acids in the pore have been proposed to serve critical roles in electrostatic attraction and binding of the permeant ions, and are determinants of ion translocation in Na_V [35, 111, 115, 120]. It has also been proposed that the negative charged aspartate at position 1539 may electrostatically maintain the pore structure by stabilizing the interaction between the selectivity filter residues in DI and DIII, which are important in channel permeability [105]. The amino acid substitution that resulted

in charge neutralization in WC may therefore have caused the decrease in the permeability ratio. In addition, the substitution of glycine at position 1540 has been previously shown to affect ion selectivity by disrupting the movement of the P-regions that induces the conformational change during opening, thereby disrupting the pore structure, ion coordination, selectivity, and permeation [115]. Although the structure of this crucial part of the pore is still a controversial issue, changes in ion selectivity and permeation may arise from reorientation and destabilization of the pore structure, and our results confirmed that amino acid residues in the P-region of DIV are important in ion selectivity and permeation.

6: CONCLUSION

Our study shows that amino acid substitutions that impart TTX resistance in the garter snake *Thamnophis sirtalis* produce changes in $Na_V1.4$ gating. The voltage dependence of activation and inactivation of TTX-resistant $Na_V1.4$ channels were significantly different compared to wild type channels. The amino acid substitutions also induced changes in conductance and ion selectivity. Ion selectivity in the most TTX-resistant $Na_V1.4$ channels, Willow Creek, was significantly altered, resulting in a decreased permeability for all permeant cations. This indicates that the structural and functional components of the pore and its selectivity filter were modified by the amino acid substitutions that confer TTX-resistance in $Na_V1.4$. These data demonstrate that TTX resistance comes at a cost to channel performance caused by changes in the gating properties and ion selectivity of the TTX resistant $Na_V1.4$.

REFERENCE LIST

1. Lee, C. H.; Ruben, P. C., Interaction between voltage-gated sodium channels and the neurotoxin, tetrodotoxin. *Channels (Austin, Tex.)* **2008,** 2, (6).
2. Catterall, W. A., From Ionic Currents to Molecular Mechanisms The Structure and Function of Voltage-Gated Sodium Channels. *Neuron* **2000,** 26, (1), 13-25.
3. Goldin, A. L.; Barchi, R. L.; Caldwell, J. H.; Hofmann, F.; Howe, J. R.; Hunter, J. C.; Kallen, R. G.; Mandel, G.; Meisler, M. H.; Netter, Y. B.; Noda, M.; Tamkun, M. M.; Waxman, S. G.; Wood, J. N.; Catterall, W. A., Nomenclature of voltage-gated sodium channels. *Neuron* **2000,** 28, (2), 365-8.
4. Catterall, W. A.; Goldin, A. L.; Waxman, S. G., International Union of Pharmacology. XLVII. Nomenclature and structure-function relationships of voltage-gated sodium channels. *Pharmacol Rev* **2005,** 57, (4), 397-409.
5. Yasumoto, T.; Murata, M., Marine toxins. *Chemical reviews* **1993,** 93, (5), 1897-1909.
6. Narahashi, T.; Moore, J. W.; Poston, R. N., Tetrodotoxin derivatives: chemical structure and blockage of nerve membrane conductance. *Science (New York, N.Y.)* **1967,** 156, (3777), 976-979.
7. Miyazawa, K.; Noguchi, T., DISTRIBUTION AND ORIGIN OF TETRODOTOXIN. *Toxin Reviews* **2005,** 20, (1), 11-33.
8. Kaneko, Y.; Matsumoto, G.; Hanyu, Y., TTX Resistivity of Na^+ Channel in Newt Retinal Neuron. *Biochemical and biophysical research communications* **1997,** 240, (3), 651-656.
9. Yotsu-Yamashita, M.; Nishimori, K.; Nitanai, Y.; Isemura, M.; Sugimoto, A.; Yasumoto, T., Binding properties of (3)H-PbTx-3 and (3)H-saxitoxin to brain membranes and to skeletal muscle membranes of puffer fish Fugu pardalis and the primary structure of a voltage-gated Na(+) channel alpha-subunit (fMNa1) from skeletal muscle of F. pardalis. *Biochem Biophys Res Commun* **2000,** 267, (1), 403-12.
10. Venkatesh, B.; Lu, S. Q.; Dandona, N.; See, S. L.; Brenner, S.; Soong, T. W., Genetic Basis of Tetrodotoxin Resistance in Pufferfishes. *Current Biology* **2005,** 15, (22), 2069-2072.
11. Maruta, S.; Yamaoka, K.; Yotsu-Yamashita, M., Two critical residues in p-loop regions of puffer fish Na^+ channels on TTX sensitivity. *Toxicon* **2007**.

12. Jost, M. C.; Hillis, D. M.; Lu, Y.; Kyle, J. W.; Fozzard, H. A.; Zakon, H. H., Toxin-resistant sodium channels: parallel adaptive evolution across a complete gene family. *Mol Biol Evol* **2008,** 25, (6), 1016-24.

13. Geffeney, S. L.; Fujimoto, E.; Brodie, E. D.; Brodle, E. D.; Ruben, P. C., Evolutionary diversification of TTX-resistant sodium channels in a predator-prey interaction. *Nature(London)* **2005,** 434, (7034), 759-763.

14. Bricelj, V. M.; Connell, L.; Konoki, K.; Macquarrie, S. P.; Scheuer, T.; Catterall, W. A.; Trainer, V. L., Sodium channel mutation leading to saxitoxin resistance in clams increases risk of PSP. *Nature* **2005,** 434, (7034), 763-767.

15. Isom, L. L.; De Jongh, K. S.; Patton, D. E.; Reber, B. F.; Offord, J.; Charbonneau, H.; Walsh, K.; Goldin, A. L.; Catterall, W. A., Primary structure and functional expression of the beta 1 subunit of the rat brain sodium channel. *Science* **1992,** 256, (5058), 839-42.

16. Davis, T. H.; Chen, C.; Isom, L. L., Sodium Channel {beta}1 Subunits Promote Neurite Outgrowth in Cerebellar Granule Neurons. *Journal of Biological Chemistry* **2004,** 279, (49), 51424-51432.

17. Noda, M.; Shimizu, S.; Tanabe, T.; Takai, T.; Kayano, T.; Ikeda, T.; Takahashi, H.; Nakayama, H.; Kanaoka, Y.; Minamino, N., Primary structure of Electrophorus electricus sodium channel deduced from cDNA sequence. *Nature* **1984,** 312, (5990), 121-127.

18. Yu, F. H.; Catterall, W. A., Overview of the voltage-gated sodium channel family. *Genome biology* **2003,** 4, (3), 207.

19. Bezanilla, F., Voltage Sensor Movements. In Rockefeller Univ Press: 2002; Vol. 120, pp 465-473.

20. Armstrong, C. M.; Bezanilla, F., Currents related to movement of the gating particles of the sodium channels. *Nature* **1973,** 242, (5398), 459-461.

21. Kontis, K. J.; Rounaghi, A.; Goldin, A. L., Sodium channel activation gating is affected by substitutions of voltage sensor positive charges in all four domains. *J Gen Physiol* **1997,** 110, (4), 391-401.

22. Stuhmer, W.; Conti, F.; Suzuki, H.; Wang, X. D.; Noda, M.; Yahagi, N.; Kubo, H.; Numa, S., Structural parts involved in activation and inactivation of the sodium channel. *Nature* **1989,** 339, (6226), 597-603.

23. Chanda, B.; Bezanilla, F., Tracking Voltage-dependent Conformational Changes in Skeletal Muscle Sodium Channel during Activation. *The Journal of General Physiology* **2002,** 120, (5), 629-645.

24. Chanda, B.; Asamoah, O. K.; Bezanilla, F., Coupling Interactions between Voltage Sensors of the Sodium Channel as Revealed by Site-specific Measurements. *The Journal of General Physiology* **2004,** 123, (3), 217-230.

25. Jones, D. K.; Ruben, P. C., Biophysical defects in voltage-gated sodium channels associated with long QT and Brugada syndromes. *Channels (Austin, Tex.)* **2008,** 2, (2).

26. Richmond, J. E.; VanDeCarr, D.; Featherstone, D. E.; George, A. L.; Ruben, P. C., Defective fast inactivation recovery and deactivation account for sodium channel myotonia in the I1160V mutant. *Biophysical journal* **1997,** 73, (4), 1896-1903.

27. Vilin, Y. Y.; Ruben, P. C., Slow inactivation in voltage-gated sodium channels: molecular substrates and contributions to channelopathies. *Cell Biochem Biophys* **2001,** 35, (2), 171-90.

28. Goldin, A. L., Mechanisms of sodium channel inactivation. *Curr Opin Neurobiol* **2003,** 13, (3), 284-90.

29. Pathak, M.; Kurtz, L.; Tombola, F.; Isacoff, E., The cooperative voltage sensor motion that gates a potassium channel. *Journal of General Physiology* **2004,** 125, (1), 57.

30. Ruben, P. C.; Starkus, J. G.; Rayner, M. D., Holding potential affects the apparent voltage-sensitivity of sodium channel activation in crayfish giant axons. *Biophys. J.* **1990,** 58, 1169-1181.

31. Ruben, P. C.; Starkus, J. G.; Rayner, M. D., Steady-state availability of sodium channels. Interactions between activation and slow inactivation. *Biophys. J.* **1992,** 61, 941-955.

32. Hayward, L. J.; Brown, R. H.; Cannon, S. C., Slow inactivation differs among mutant Na channels associated with myotonia and periodic paralysis. *Biophysical journal* **1997,** 72, (3), 1204-1219.

33. Xiong, W.; Farukhi, Y. Z.; Tian, Y.; DiSilvestre, D.; Li, R. A.; Tomaselli, G. F., A conserved ring of charge in mammalian Na channels: a molecular regulator of the outer pore conformation during slow inactivation. *The Journal of physiology* **2006,** 576, (3), 739-754.

34. Vilin, Y. Y.; Fujimoto, E.; Ruben, P. C., A single residue differentiates between human cardiac and skeletal muscle Na^+ channel slow inactivation. *Biophys J* **2001,** 80, (5), 2221-30.

35. Terlau, H.; Heinemann, S. H.; Stuhmer, W.; Pusch, M.; Conti, F.; Imoto, K.; Numa, S., Mapping the site of block by tetrodotoxin and saxitoxin of sodium channel II. *FEBS letters* **1991,** 293, (1-2), 93-96.

36. Noda, M.; Suzuki, H.; Numa, S.; Stuhmer, W., A single point mutation confers tetrodotoxin and saxitoxin insensitivity on the sodium channel II. *FEBS letters* **1989,** 259, (1), 213-216.

37. Penzotti, J. L.; Fozzard, H. A.; Lipkind, G. M.; Dudley, S. C., Jr., Differences in saxitoxin and tetrodotoxin binding revealed by mutagenesis of the Na^+ channel outer vestibule. *Biophysical journal* **1998,** 75, (6), 2647-2657.

38. Satin, J.; Kyle, J. W.; Chen, M.; Bell, P.; Cribbs, L. L.; Fozzard, H. A.; Rogart, R. B., A mutant of TTX-resistant cardiac sodium channels with TTX-sensitive properties. *Science* **1992,** 256, (5060), 1202-5.

39. Cummins, T. R.; Dib-Hajj, S. D.; Black, J. A.; Akopian, A. N.; Wood, J. N.; Waxman, S. G., A Novel Persistent Tetrodotoxin-Resistant Sodium Current In SNS-Null And Wild-Type Small Primary Sensory Neurons. In *Journal of Neuroscience*, Soc Neuroscience: 1999; Vol. 19, pp 43-43.

40. Tomaselli, G. F.; Chiamvimonvat, N.; Nuss, H. B.; Balser, J. R.; Perez-Garcia, M. T.; Xu, R. H.; Orias, D. W.; Backx, P. H.; Marban, E., A mutation in the pore of the sodium channel alters gating. *Biophysical journal* **1995,** 68, (5), 1814-1827.

41. Hilber, K.; Sandtner, W.; Kudlacek, O.; Glaaser, I. W.; Weisz, E.; Kyle, J. W.; French, R. J.; Fozzard, H. A.; Dudley, S. C.; Todt, H., The Selectivity Filter of the Voltage-gated Sodium Channel Is Involved in Channel Activation. *Journal of Biological Chemistry* **2001,** 276, (30), 27831-27839.

42. Doyle, D. A.; Cabral, J. M.; Pfuetzner, R. A.; Kuo, A.; Gulbis, J. M.; Cohen, S. L.; Chait, B. T.; MacKinnon, R., The structure of the potassium channel: molecular basis of K^+ conduction and selectivity. *Science* **1998,** 280, (5360), 69.

43. Striessnig, J.; Glossmann, H.; Catterall, W. A., Identification of a phenylalkylamine binding region within the alpha 1 subunit of skeletal muscle Ca2 channels. *Proceedings of the National Academy of Sciences of the United States of America* **1990,** 87, (23), 9108.

44. Guy, H. R.; Seetharamulu, P., Molecular Model of the Action Potential Sodium Channel. *Proceedings of the National Academy of Sciences of the United States of America* **1986,** 83, (2), 508-512.

45. Hilber, K.; Sandtner, W.; Zarrabi, T.; Zebedin, E.; Kudlacek, O.; Fozzard, H. A.; Todt, H., Selectivity Filter Residues Contribute Unequally to Pore Stabilization in Voltage-Gated Sodium Channels. *Biochemistry* **2005,** 44, (42), 13874-13882.

46. Lipkind, G. M.; Fozzard, H. A., KcsA crystal structure as framework for a molecular model of the Na(+) channel pore. *Biochemistry* **2000,** 39, (28), 8161-70.

47. Sato, C.; Ueno, Y.; Asai, K.; Takahashi, K.; Sato, M.; Engel, A.; Fujiyoshi, Y., The voltage-sensitive sodium channel is a bell-shaped molecule with several cavities. *Nature* **2001,** 409, (6823), 1047-51.

48. Ogata, N.; Yoshida, S., New Perspectives on the Structure and Function of the Na^+ Channel Multigene Family. *CURRENT MEDICINAL CHEMISTRY CENTRAL NERVOUS SYSTEM AGENTS* **2002,** 2, (1), 59-82.

49. Clare, J. J.; Tate, S. N.; Nobbs, M.; Romanos, M. A., Voltage-gated sodium channels as therapeutic targets. *Drug discovery today* **2000,** 5, (11), 506-520.

50. Meadows, L. S.; Chen, Y. H.; Powell, A. J.; Clare, J. J.; Ragsdale, D. S., Functional modulation of human brain Nav1.3 sodium channels, expressed in mammalian cells, by auxiliary beta 1, beta 2 and beta 3 subunits. *Neuroscience* **2002,** 114, (3), 745-53.

51. Klugbauer, N.; Lacinova, L.; Flockerzi, V.; Hofmann, F., Structure and functional expression of a new member of the tetrodotoxin-sensitive voltage-activated sodium channel family from human neuroendocrine cells. *The EMBO journal* **1995,** 14, (6), 1084-90.

52. Chahine, M.; Bennett, P. B.; George, A. L., Jr.; Horn, R., Functional expression and properties of the human skeletal muscle sodium channel. *Pflugers Arch* **1994,** 427, (1-2), 136-42.

53. Smith, M. R.; Smith, R. D.; Plummer, N. W.; Meisler, M. H.; Goldin, A. L., Functional analysis of the mouse Scn8a sodium channel. *J Neurosci* **1998,** 18, (16), 6093-102.

54. Gellens, M. E.; George, A. L., Jr.; Chen, L. Q.; Chahine, M.; Horn, R.; Barchi, R. L.; Kallen, R. G., Primary structure and functional expression of the human cardiac tetrodotoxin-insensitive voltage-dependent sodium channel. *Proc Natl Acad Sci U S A* **1992,** 89, (2), 554-8.

55. George, A. L., Jr.; Varkony, T. A.; Drabkin, H. A.; Han, J.; Knops, J. F.; Finley, W. H.; Brown, G. B.; Ward, D. C.; Haas, M., Assignment of the human heart tetrodotoxin-resistant voltage-gated Na^+ channel alpha-subunit gene (SCN5A) to band 3p21. *Cytogenetics and cell genetics* **1995,** 68, (1-2), 67-70.

56. Akopian, A. N.; Sivilotti, L.; Wood, J. N., A tetrodotoxin-resistant voltage-gated sodium channel expressed by sensory neurons. *Nature* **1996,** 379, (6562), 257-62.

57. Backx, P. H.; Yue, D. T.; Lawrence, J. H.; Marban, E.; Tomaselli, G. F., Molecular localization of an ion-binding site within the pore of mammalian sodium channels. *Science* **1992,** 257, (5067), 248-251.

58. Waxman, S. G.; Kocsis, J. D.; Black, J. A., Type III sodium channel mRNA is expressed in embryonic but not adult spinal sensory neurons, and is reexpressed following axotomy. *Journal of Neurophysiology* **1994,** 72, (1), 466-470.

59. Dib-Hajj, S. D.; Fjell, J.; Cummins, T. R.; Zheng, Z.; Fried, K.; Lamotte, R.; Black, J. A.; Waxman, S. G., Plasticity of sodium channel expression in DRG neurons in the chronic constriction injury model of neuropathic pain. *Pain(Amsterdam)* **1999,** 83, (3), 591-600.

60. Hains, B. C.; Saab, C. Y.; Klein, J. P.; Craner, M. J.; Waxman, S. G., Altered Sodium Channel Expression in Second-Order Spinal Sensory

Neurons Contributes to Pain after Peripheral Nerve Injury. *Journal of Neuroscience* **2004,** 24, (20), 4832-4839.

61. Yoshida, S., Tetrodotoxin-resistant sodium channels. *Cellular and molecular neurobiology* **1994,** 14, (3), 227-44.

62. Momin, A.; Wood, J. N., Sensory neuron voltage-gated sodium channels as analgesic drug targets. *Current Opinion in Neurobiology* **2008**.

63. Catterall, W. A.; Cestéle, S.; Yarov-Yarovoy, V.; Yu, F. H.; Konoki, K.; Scheuer, T., Voltage-gated ion channels and gating modifier toxins. *Toxicon* **2007,** 49, (2), 124-141.

64. Al-Sabi, A.; McArthur, J.; Ostroumov, V.; French, R. J., Marine Toxins That Target Voltage-gated Sodium Channels. *Mar.Drugs* **2006,** 4, 157-192.

65. Catterall, W. A.; Risk, M., Toxin T4 (6) from Ptychodiscus brevis (formerly Gymnodinium breve) enhances activation of voltage-sensitive sodium channels by veratridine. *Molecular pharmacology* **1981,** 19, (2), 345.

66. Lombet, A.; Bidard, J. N.; Lazdunski, M., Ciguatoxin and brevetoxins share a common receptor site on the neuronal voltage-dependent Na^+ channel. *FEBS letters* **1987,** 219, (2), 355.

67. Jonas, P.; Vogel, W.; Arantes, E. C.; Giglio, J. R., Toxin of the scorpionTityus serrulatus modifies both activation and inactivation of sodium permeability of nerve membrane. *Pflügers Archiv European Journal of Physiology* **1986,** 407, (1), 92-99.

68. Nakayama, H.; Hatanaka, Y.; Yoshida, E.; Oka, K.; Takanohashi, M.; Amano, Y.; Kanaoka, Y., Photolabeled sites with a tetrodotoxin derivative in the domain III and IV of the electroplax sodium channel. **1992,** 184, 900-907.

69. Guillory, R. J.; Rayner, M. D.; D'Arrigo, J. S., Covalent labeling of the tetrodotoxin receptor in excitable membranes. *Science* **1977,** 196, (4292), 883-885.

70. Lipkind, G. M.; Fozzard, H. A., A structural model of the tetrodotoxin and saxitoxin binding site of the Na channel. *Biophysical journal* **1994,** 66, (1), 1-13.

71. Hille, B., Charges and Potentials at the Nerve Surface Divalent ions and pH. *The Journal of general physiology* **1968,** 51, (2), 221-236.

72. Shrager, P.; Profera, C., Inhibition of the receptor for tetrodotoxin in nerve membranes by reagents modifying carboxyl groups. *Biochimica et biophysica acta* **1973,** 318, (1), 141-146.

73. Henderson, R.; Ritchie, J. M.; and, G. R. S., Evidence That Tetrodotoxin and Saxitoxin Act at a Metal Cation Binding Site in the Sodium Channels of Nerve Membrane. *Proceedings of the National Academy of Sciences* **1974,** 71, (10), 3936-3940.

74. Hille, B., The receptor for tetrodotoxin and saxitoxin. A structural hypothesis. *Biophysical journal* **1975,** 15, (6), 615.

75. Choudhary, G.; Yotsu-Yamashita, M.; Shang, L.; Yasumoto, T.; Dudley, S. C., Interactions of the C-11 Hydroxyl of Tetrodotoxin with the Sodium Channel Outer Vestibule. *Biophysical journal* **2003,** 84, (1), 287-294.

76. Patton, D. E.; Goldin, A. L., A voltage-dependent gating transition induces use-dependent block by tetrodotoxin of rat IIA sodium channels expressed in Xenopus oocytes. *Neuron* **1991,** 7, (4), 637-47.

77. Dumaine, R.; Hartmann, H. A., Two conformational states involved in the use-dependent TTX blockade of human cardiac Na^+ channel. *American Journal of Physiology- Heart and Circulatory Physiology* **1996,** 270, (6), 2029-2037.

78. Soong, T. W.; Venkatesh, B., Adaptive evolution of tetrodotoxin resistance in animals. *Trends in genetics : TIG* **2006,** 22, (11), 621-626.

79. Matsumura, K., Tetrodotoxin as a pheromone. *Nature* **1995,** 378, (6557), 563-564.

80. Brodie, E. D.; Ridenhour, B. J., THE EVOLUTIONARY RESPONSE OF PREDATORS TO DANGEROUS PREY: HOTSPOTS AND COLDSPOTS IN THE GEOGRAPHIC MOSAIC OF COEVOLUTION BETWEEN GARTER SNAKES AND NEWTS. *Evolution* **2002,** 56, (10), 2067-2082.

81. Heggeness, S. T.; Starkus, J. G., Saxitoxin and tetrodotoxin. Electrostatic effects on sodium channel gating current in crayfish axons. *Biophysical journal* **1986,** 49, (3), 629-643.

82. Brodie Jr, E. D.; Hensel Jr, J. L.; Johnson, J. A., Toxicity of the urodele amphibians Taricha, Notophthalmus, Cynops and Paramesotriton (salamandridae). *Copeia* **1974**, 506-511.

83. Brodie Iii, E. D.; Brodie Jr, E. D., Tetrodotoxin resistance in garter snakes: an evolutionary response of predators to dangerous prey. *Evolution* **1990**, 651-659.

84. Brodie Iii, E. D.; Brodie Jr, E. D., Evolutionary response of predators to dangerous prey: reduction of toxicity of newts and resistance of garter snakes in island populations. *Evolution* **1991**, 221-224.

85. Brodie Iii, E. D.; Brodie Jr, E. D., Predator-prey arms races. *Bioscience* **1999,** 49, (7), 557-568.

86. Geffeney, S.; Brodie, E. D., Jr.; Ruben, P. C.; Brodie, E. D., 3rd, Mechanisms of adaptation in a predator-prey arms race: TTX-resistant sodium channels. *Science* **2002,** 297, (5585), 1336-9.

87. Janzen, F. J.; Krenz, J. G.; Haselkorn, T. S.; Brodie, E. D., Molecular phylogeography of common garter snakes (Thamnophis sirtalis) in western North America: implications for regional historical forces. *Molecular ecology* **2002,** 11, (9), 1739-1751.

88. Swofford, D. L., Phylogenetic analysis using parsimony, version 4.0 b4a. *Ilinois Natural History Survey, Champaign, USA* **2000**.

89. Jayne, B. C.; Bennett, A. F., Selection on locomotor performance capacity in a natural population of garter snakes. *Evolution* **1990,** 44, (5), 1204-1229.

90. Sun, H.; Varela, D.; Chartier, D.; Ruben, P. C.; Nattel, S.; Zamponi, G. W.; Leblanc, N., Differential Interactions of Na^+ Channel Toxins with T-type Ca^{2+} Channels. *The Journal of general physiology* **2008,** 132, (1), 101.

91. Wang, J. Z.; Rojas, C. V.; Zhou, J. H.; Schwartz, L. S.; Nicholas, H.; Hoffman, E. P., Sequence and genomic structure of the human adult skeletal muscle sodium channel alpha subunit gene on 17q. *Biochemical and biophysical research communications* **1992,** 182, (2), 794.

92. Strausberg, R. L.; Feingold, E. A.; Grouse, L. H.; Derge, J. G.; Klausner, R. D.; Collins, F. S.; Wagner, L.; Shenmen, C. M.; Schuler, G. D.; Altschul, S. F., Generation and initial analysis of more than 15,000 full-length human and mouse cDNA sequences. *Proceedings of the National Academy of Sciences of the United States of America* **2002,** 99, (26), 16899.

93. Santarelli, V. P.; Eastwood, A. L.; Dougherty, D. A.; Horn, R.; Ahern, C. A., A cation- interaction discriminates among sodium channels that are either sensitive or resistant to tetrodotoxin block. *Journal of Biological Chemistry* **2007,** 282, (11), 8044.

94. Stefani, E.; Bezanilla, F., Cut-open oocyte voltage-clamp technique. *Methods in enzymology* **1998,** 293, 300.

95. Favre, I.; Moczydlowski, E.; Schild, L., On the structural basis for ionic selectivity among Na^+, K^+, and Ca^{2+} in the voltage-gated sodium channel. *Biophysical journal* **1996,** 71, (6), 3110-3125.

96. Pérez-García, M. T.; Chiamvimonvat, N.; Ranjan, R.; Balser, J. R.; Tomaselli, G. F.; Marban, E., Mechanisms of sodium/calcium selectivity in sodium channels probed by cysteine mutagenesis and sulfhydryl modification. *Biophysical journal* **1997,** 72, (3), 989-996.

97. Pérez-García, M. T.; Chiamvimonvat, N.; Marban, E.; Tomaselli, G. F., Structure of the sodium channel pore revealed by serial cysteine mutagenesis. In National Acad Sciences: 1996; Vol. 93, pp 300-304.

98. Hille, B., The permeability of the sodium channel to organic cations in myelinated nerve. *Journal of General Physiology* **1971,** 58, (6), 599-619.

99. Hille, B., *Ion channels of excitable membranes/Bertil Hille*. Sinauer Associates, Inc.: 2001.

100. Shcherbatko, A.; Ono, F.; Mandel, G.; Brehm, P., Voltage-Dependent Sodium Channel Function Is Regulated Through Membrane Mechanics. *Biophysical journal* **1999,** 77, (4), 1945-1959.

101. Featherstone, D. E.; Richmond, J. E.; Ruben, P. C., Interaction between fast and slow inactivation in Skm1 sodium channels. *Biophys J* **1996,** 71, (6), 3098-109.

102. Pauling, L., *The nature of the chemical bond and the structure of molecules and crystals: An introduction to modern structural chemistry*. Cornell Univ Pr: 1960.

103. Chang, N. S.; French, R. J.; Lipkind, G. M.; Fozzard, H. A.; Dudley Jr, S., Predominant Interactions between [mu]-Conotoxin Arg-13 and the Skeletal Muscle Na^+ Channel Localized by Mutant Cycle Analysis. *Biochemistry* **1998,** 37, (13), 4407-4419.

104. Todt, H.; Dudley, S. C.; Kyle, J. W.; French, R. J.; Fozzard, H. A., Ultra-slow inactivation in 1 Na^+ channels is produced by a structural rearrangement of the outer vestibule. *Biophysical journal* **1999,** 76, (3), 1335-1345.

105. Hilber, K.; Sandtner, W.; Zarrabi, T.; Zebedin, E.; Kudlacek, O.; Fozzard, H. A.; Todt, H., Selectivity Filter Residues Contribute Unequally to Pore Stabilization in Voltage-Gated Sodium Channels. *Biochemistry* **2005,** 44, (42), 13874-13882.

106. Horn, R.; Ding, S.; Gruber, H. J., Immobilizing the moving parts of voltage-gated ion channels. *Journal of General Physiology* **2000,** 116, (3), 461-476.

107. Armstrong, C. M., Na channel inactivation from open and closed states. *Proceedings of the National Academy of Sciences* **2006,** 103, (47), 17991.

108. Bezanilla, F., How membrane proteins sense voltage. *Nature Reviews Molecular Cell Biology* **2008,** 9, (4), 323-332.

109. Mitrovic, N.; George, A. L.; Horn, R., Role of domain 4 in sodium channel slow inactivation. *Journal of General Physiology* **2000,** 115, (6), 707-718.

110. Khan, A.; Romantseva, L.; Lam, A.; Lipkind, G.; Fozzard, H. A., Role of outer ring carboxylates of the rat skeletal muscle sodium channel pore in proton block. *The Journal of physiology* **2002,** 543, (1), 71-84.

111. Chiamvimonvat, N.; Perez-Garcia, M. T.; Tomaselli, G. F.; Marban, E., Control of ion flux and selectivity by negatively charged residues in the outer mouth of rat sodium channels. *The Journal of physiology* **1996,** 491, (1), 51-59.

112. Benitah, J. P.; Ranjan, R.; Yamagishi, T.; Janecki, M.; Tomaselli, G. F.; Marban, E., Molecular motions within the pore of voltage-dependent sodium channels. *Biophysical journal* **1997,** 73, (2), 603-613.

113. Benitah, J. P.; Chen, Z.; Balser, J. R.; Tomaselli, G. F.; Marban, E., Molecular dynamics of the sodium channel pore vary with gating: interactions between P-segment motions and inactivation. *Journal of Neuroscience* **1999,** 19, (5), 1577.

114. Ong, B. H.; Tomaselli, G. F.; Balser, J. R., A structural rearrangement in the sodium channel pore linked to slow inactivation and use dependence. *The Journal of general physiology* **2000,** 116, (5), 653.

115. Tsushima, R. G.; Li, R. A.; Backx, P. H., Altered Ionic Selectivity of the Sodium Channel Revealed by Cysteine Mutations within the Pore. *J. Gen. Physiol.* **1997,** 109, (4), 463-475.

116. Yang, Y. C.; Hsieh, J. Y.; Kuo, C. C., The external pore loop interacts with S6 and S3-S4 linker in domain 4 to assume an essential role in gating control and anticonvulsant action in the Na^+ channel. *Journal of General Physiology* **2009,** 134, (2), 95.

117. Featherstone, D. E.; Fujimoto, E.; Ruben, P. C., A defect in skeletal muscle sodium channel deactivation exacerbates hyperexcitability in human paramyotonia congenita. *The Journal of physiology* **1998,** 506, (3), 627.

118. Cannon, S. C.; Strittmatter, S. M., Functional expression of sodium channel mutations identified in families with periodic paralysis. *Neuron* **1993,** 10, (2), 317.

119. Vedantham, V.; Cannon, S. C., Rapid and slow voltage-dependent conformational changes in segment IVS6 of voltage-gated Na^+ channels. *Biophysical journal* **2000,** 78, (6), 2943-2958.

120. Hille, B., The permeability of the sodium channel to metal cations in myelinated nerve. *Journal of General Physiology* **1972,** 59, (6), 637-658.